Occurrence and mobility of major and trace elements in groundwater from pristine volcanic aquifers in Jeju Island, Korea

Dong-Chan Koh [a, b, *], Gi-Tak Chae [a], Jong-Sik Ryu [c], Seung-Gu Lee [a], Kyung-Seok Ko [a, b]

[a] Korea Institute of Geoscience and Mineral Resources, 124 Gwahang-no, Yuseong-gu, Daejeon 305-350, Republic of Korea
[b] University of Science and Technology, 217 Gajeong-ro, Yuseong-gu, Daejeon 305-333, Republic of Korea
[c] Division of Earth and Environmental Sciences, Korea Basic Science Institute, Chungbuk 363-883, Republic of Korea

ABSTRACT

Major and trace elements in groundwater from basaltic aquifers in pristine conditions were investigated in a volcanic island to evaluate sources, sinks, and mobility of elements over a wide range of mineralization conditions with total dissolved solids from 50 mg/L to 3400 mg/L. Groundwater was highly undersaturated with respect to primary silicate minerals, indicating that dissolution of basaltic rocks may continue under conditions with precipitation of calcite and secondary silicates. Evolution of B/Cl ratio in groundwater from marine aerosols to basaltic rocks showed that the ratio could be used as a conservative tracer for interactions between water and basaltic rocks. Relative mobility (RM) of elements calculated using the concentrations of elements in the local basaltic rocks and those in groundwater showed that mobility decreased in the order of B > Rb > Na > K > Mg > Ca > Mo > V > Si > Sr > Sc > P > U > Zn > Pb > Cr > Cu > Ba > Ni > Ti > (Mn, Al, Fe, Co, Th) indicating that oxyanion-forming elements and alkali metals had the highest mobility. Compared to average RM, V had decreased mobility, and Fe and Mn had increased mobility in anoxic groundwater while V, Mo, and U had higher mobility in oxic-alkaline water. The sources of V, Cr, Cu, and Zn in rocks were estimated using the partition coefficients between minerals and basaltic melt, and the disparity between sources and mobility indicated that sinks are more important for controlling the concentrations of these elements in groundwater than the contents in the rocks. Principal component analysis (PCA) of hydrogeochemical parameters in groundwater produced three principal components (PC) which represent dissolution of basaltic rocks without significant attenuation of released solutes, higher degree of water–rock interactions resulting in oxic-alkaline conditions, and attenuation of Zn and Cu in higher pH, respectively. Spatial distribution of PCs revealed that groundwater with elevated concentrations of mobile elements was concentrated in the southwestern area and that concentrations of V and Cr were more scattered, which is likely to be controlled by pH and redox states of groundwater as well as degree of water–rock interactions.

1. Introduction

Basaltic rocks have a considerable number of solid phases with high dissolution rates, including olivine, glass, and pyroxenes. Both field and laboratory studies have shown that the chemical composition of surface and groundwater can be significantly affected by basaltic rocks, due to their high reactivity during water–rock interactions (Meybeck, 1987; Bluth and Kump, 1994). The hydrogeochemistry of natural water in basaltic rocks has been widely investigated in terms of the chemical weathering and mobility of elements (Louvat and Allegre, 1997; Stefansson and Gislason, 2001). The chemical composition of natural water in Iceland was studied in terms of the thermodynamic equilibrium between primary silicate minerals and water (Gislason and Arnorsson, 1993; Stefansson et al., 2001), and the rate of chemical weathering in basaltic terrains (Gislason and Eugster, 1987; Stefansson and Gislason, 2001). Pokrovsky et al. (2005) determined the rate of chemical weathering of basalts and element mobility by combining a chemical and mineralogical analysis of solids and the chemistry of natural water in Central Siberia.

For the active volcanic area of Mt. Etna in Italy, studies involving the sources of solutes, water quality, mobility, and thermodynamic

---

* Corresponding author. Korea Institute of Geoscience and Mineral Resources, 124 Gwahang-no, Yuseong-gu, Daejeon 305-350, Republic of Korea.
E-mail address: chankoh@kigam.re.kr (D.-C. Koh).

modeling were conducted around the volcano where groundwater is affected by inputs of CO_2-rich magmatic gas and changes in the volcanic plumbing system (Giammanco et al., 1998; Aiuppa et al., 2000a, 2003). The groundwater quality of volcanic aquifers is important because the dissolution of aquifer materials can provide elevated levels of dissolved constituents. Some studies of major and minor elements in groundwater have been conducted to determine chemical weathering and groundwater quality (Edmunds et al., 2002; Van Der Weijden and Pacheco, 2003). However, the behavior of dissolved trace elements in groundwater in volcanic areas where the volcano is inactive has not been investigated extensively.

In this study, the behavior of major and trace elements in pristine groundwater from Quaternary basaltic rocks with various levels of water–rock interactions is investigated on a volcanic island with negligible historic signature of volcanic and geothermal activity. The aims of this study are: 1) to characterize the variation of the dissolved concentrations of major and trace elements due to water–rock interactions, 2) to evaluate their geochemical mobility and determine the possible sources and sinks of the elements in groundwater, and 3) to provide baseline groundwater quality of volcanic aquifers which are the sole source of drinking water on the island where significant land use changes are expected due to higher development pressure.

2. Study area

2.1. Geologic and hydrogeologic setting

The study area is a 589 km^2 mountainous region (200–600 m a.s.l.) of Jeju Island, Korea, corresponding to 32% of total surface area of the island (Fig. 1). The island was formed by Quaternary basaltic and trachytic volcanism from 1.2 Ma to 0.025 Ma. The island has no active volcanoes at present (Park and Kwon, 1993a). The basaltic rocks consist of numerous lava flows and cover most of the surface area of the island, which are highly permeable and form the principal aquifers (Koh et al., 2005a). The basaltic rocks are underlain by the Seogwipo Formation which consists of consolidated

or semi-consolidated hydrovolcanic tuffs (Sohn et al., 2002). The basement rock on the island consists of pyroclastic rocks, welded tuff, lapilli tuff, and granite (Koh et al., 2005a). In the eastern part of Jeju, basaltic rocks are found at sea level whereas the Seogwipo Formation is present near sea level in other areas that have upward slopes toward the center of the island (Won et al., 2006).

The land use of the study area is mainly natural cover and pasture. Groundwater of the area is much less affected by anthropogenic activities and the direct effect of seawater intrusion is not observed (Koh et al., 2009). Park et al. (2014) showed that 69% of the total recharge occurred in the elevation over 200 m using a distributed water balance model, which indicates the mountainous region would be a critical groundwater recharge zone. The land use of the island has undergone dramatic changes in the coastal area (<200 m a.s.l.) and proportion of anthropogenic land uses increased from 41% in 1980 to 73% in 2000. The anthropogenic land uses of agricultural and recreational areas also affected the mountainous region and their proportion increased from 3% in 1980 to 21% in 2000 though much of them are concentrated near the boundary of the coastal and mountainous region (Ha et al., 2009). Considering this temporal trend in land use patterns, groundwater quality in the mountainous region may be adversely affected by the change in the near future.

2.2. Mineralogic and chemical composition of basaltic rocks

Park et al. (1999) compiled data regarding the concentrations of the major elements in the whole rocks of Jeju Island, and showed that the majority of basaltic rocks correspond to basalt and trachybasalt. Based on the classification of alkalic and sub-alkalic basalts, it was confirmed that alkali basalts are predominant and tholeiitic basalts are only found in coastal areas. The results of a modal analysis of the basaltic rocks showed that plagioclase (An$_{45-65}$) is the most abundant mineral comprising 60 vol. % (Won, 1976). The average volume percentage of the groundmass with crystal sizes smaller than 0.1 mm is 85% and for phenocrysts (plagioclase, olivine, clinopyroxenes, and titanomagnetite) the values are 10.7, 2.4, 1.4, and 0.2%, respectively. The groundmass includes lath-type

Fig. 1. Location map of groundwater sampling sites. Location of a borehole where rock samples for chemical analysis of B and Cl were taken are shown as "X" mark in the southwestern part of the study area.

plagioclase and microcrystalline olivine, pyroxenes, and titano-magnetite with small amounts of glass filling the interstices between microcrystalline minerals (Park and Kwon, 1993a).

The major and trace element content of local basaltic rocks was compiled from the published literature on Jeju Island (Park and Kwon, 1993a, 1993b; Lee et al., 1994; Park et al., 1996; Won et al., 1998; Sohn et al., 2002; Tatsumi et al., 2005), which is listed in Table 1S (Supporting Material). Compared to average basalts (Taylor, 1965), the basaltic rocks on the island have higher abundances of Na, K, and P indicating the predominance of alkali basalts. Among the trace elements, incompatible elements (Ba, Sr, Rb, and U) are enriched while most of the first transition elements (Sc, V, Cr, Co, Ni, and Cu) compatible in basaltic magma are depleted (Tatsumi et al., 2005).

3. Methods

3.1. Field investigation

A total of 52 groundwater samples were collected from 48 wells and 5 springs located higher than 200 m a.s.l. in May, 2008 (Fig. 1). The field campaign was conducted in the dry season to represent the base-flow conditions of aquifers. Most rainfall at Jeju is concentrated in the wet season from June to September (Lee et al., 1999). The study area was mainly composed of natural cover and anthropogenic contamination was not expected. However, there was an indication of nitrate contamination in some wells in the western part of the site (Koh et al., 2009). These wells were excluded from the field investigation because our study only considered natural processes on the island. Field measurements of temperature, pH, electrical conductivity (EC), dissolved oxygen (DO), and redox potential (Eh) were taken, and samples were collected when these parameters were stable. Groundwater samples were filtered through 0.2-μm membrane filters and samples for cation analysis were acidified to pH <2 in the field with ultra-pure concentrated HNO_3. Aliquots of acidified samples for trace element analysis were stored in acid-cleaned polyethylene bottles.

3.2. Chemical analysis

The major anions (Cl^-, SO_4^{2-}, NO_3^-, and F^-) were measured using ion-exchange chromatography (ICS-1500, Dionex) and Br was also measured IC with larger sample loops to detect low-level concentration. Major elements (Ca, Mg, Na, K, Si, and Fe) were measured using inductively coupled plasma atomic emission spectrometry (ICP-AES; Optima 4300DU, Perkin Elmer). Alkalinity was determined as total alkalinity using an automatic titrator (Orion 950 Titrator) with acidimetric titration to the endpoint of pH = 4.5. Charge balance errors were less than 5%, except for some low-mineral content water samples with EC < 100 μS/cm. Measured field parameters and concentrations of major elements in groundwater were shown in Table 2S (Supporting Material). Total dissolved solids (TDS) was calculated from measured major constituents (Fishman and Friedman, 1989).

A total of 33 trace elements (Li, B, Be, Al, P, Sc, Ti, V, Cr, Mn, Co, Ni, Cu, Zn, Rb, Sr, Ba, Cs, As, Se, Sb, Ga, Ge, Mo, Pb, Ag, Cd, Sn, Te, Ta, Bi, Th, and U) were measured using ICP mass spectrometry (ICP-MS; X-7 model, Thermo Elemental) at the Korea Basic Sciences Institute (Table 3S (Supporting Material)). Signal variation and matrix effects were eliminated using 1 μg/L internal standards of ^{115}In and ^{205}Tl. Precision and accuracy were regularly checked using reference materials: SLRS-4 (River water for trace metals) and NASS-5 (Seawater for trace metals). The concentrations of all analyzed elements in field blanks were below the detection limits, indicating that there was no significant contamination during sampling.

For contents of B and Cl in rocks, some rock samples were analyzed by the instrumental neutron activation analysis technique (INAA) in Korea Atomic Energy Research Institute to compared concentrations of those elements in groundwater (Table 1). The rocks samples were obtained from the drilled core of a borehole in the southwestern part of the study area (Fig. 1). The samples were taken along the depth of the core to cover various lava flows erupted during late Pleistocene in the island (Jeong et al., 2014).

3.3. Multivariate statistical analysis

Principal component analysis (PCA) was used to identify geochemical processes controlling major and trace elements in groundwater. PCA has been widely applied to interpret hydrogeochemical data of major and trace elements (Helena et al., 2000; Xie et al., 2005). The principal components were extracted from the correlation matrix of 30 hydrogeochemical parameters including temperature, pH, DO, Eh, EC, TDS, Ca, Mg, Na, K, HCO_3, Cl, SO_4, NO_3, F, SiO_2, B, Al, Ti, V, Cr, Cu, Zn, Rb, Sr, Mo, Ba, U, Sc, and P. Trace elements were excluded in the statistical analysis when proportion of measured concentrations below detection limits (DL) were greater than 30%. Concentrations below DL were assumed as half values of the DLs for the selected elements. Because most variables are highly skewed on a linear scale, logarithmic transformation was applied except for temperature and pH. The measured values had wide ranges and were based on different units, they were standardized as z-scores with a mean of zero and standard deviation of one (Koh et al., 2009). Sample D1 was excluded in the analysis because initial trial showed the sample had a clearly distinct score from those of the remaining samples.

4. Results

4.1. Water types and hydrogeochemistry of the major elements

All samples had nitrate concentration less than 7 mg/L suggesting that the effects of anthropogenic processes were minimal (Koh et al., 2009). The direct effect of seawater on dissolved solutes in groundwater was expected to be minimal because seawater intrusion has only been observed in the eastern coastal area of the island (Kim et al., 2003; Koh et al., 2007). Another source of solutes in groundwater is sea-salt spray (Moon et al., 2012). Cl concentration in rainwater was 2.6 mg/L on average which was measured at the altitude of 510 m asl. in the northern part of the island (Kang et al., 1999) and less than 10 mg/L in most of groundwater of this study (Table 2S (Supporting Material)). Furthermore, Na/Cl ratio of groundwater is well above the marine ratio even at very low level of Cl indicating Na mainly derived from the dissolution of primary minerals in basaltic rocks (Fig. 1Sa (Supporting Material)), which

Table 1
Measured concentrations of B and Cl in local basaltic rocks.

Sample	B (ppm)		Cl (ppm)		Cl/B[b]
	Conc.	S[a]	Conc.	s	
X-15A	7.0	0.4	185	8	26
X-44A	9.2	0.2	154	14	17
X-59A	12.6	0.3	1141	5	91
X-74A	8.5	0.3	126	14	15
X-104A	7.4	0.5	183	18	25
X-185A	11.7	0.4	210	3	18
X-244A	12.9	0.2	1127	6	87
Average	9.9	–	446	–	40
Std. Dev.	2.5	–	470	–	34

[a] Sample standard deviation of measured concentration.
[b] Cl/B mass ratio of atmospheric input was assumed to be that of seawater (1330).

was clearly observed in other basaltic aquifers in an island environment (Join et al., 1997; Cruz and Amaral, 2004). These suggest that effect of marine sources on concentrations of major and trace elements in groundwater are insignificant compared to water–rock interactions.

Considering hydrogeochemical characteristics, groundwater samples were classified into four groups based on TDS, HCO_3 concentration, and partial pressure of carbon dioxide (P_{CO2}): high-altitude springs (TDS < 60 mg/L, HCO_3 < 25 mg/L, EC < 60 μS/cm), low-mineral water (60 mg/L < TDS < 150 mg/L, 25 mg/L < HCO_3 < 90 mg/L, 60 μS/cm < EC < 155 μS/cm), and mineral water (TDS > 150 mg/L, HCO_3 > 90 mg/L, EC > 155 μS/cm). This classification is consistent with those suggested by Koh et al. (2009). CO_2-rich water had $P_{CO2} > 10^{-1}$ atm whereas other water types usually had $P_{CO2} < 10^{-2.5}$ atm. Mineral water was further classified as Mg-rich mineral water and Na-rich mineral water based on the concentrations of the major cations (Fig. 1Sb (Supporting Material)). The majority of the mineral water was Na-type water, which can be attributed to predominance of alkaline basaltic rocks with a high Na and K content in the island (Park et al., 1999).

High-altitude springs and low-mineral water had wide range of pH of 6.5–8.5 while mineral water have pH > 7.5, mostly >8, indicating advanced degree of water–rock interactions (Fig. 1Sc (Supporting Material)). CO_2-rich water had lower pH of about 6.3 due to higher P_{CO2}. In Jeju island, groundwater is mostly oxic (Koh et al., 2007). Dissolved oxygen (DO) is higher than 8 mg/L in high-altitude springs and low-mineral water. However, groundwater with higher TDS had much lower DO. CO_2-rich water and some of mineral water had DO less than 1 mg/L indicating effective isolation from fast recharge water (Koh et al., 2009).

With an increase in TDS, Na and Mg concentrations increased linearly in all water samples while there was a wider scatter of Ca concentrations in low-mineral water. NO_3 in low-mineral water had no clear trend with TDS. NO_3 concentrations in mineral water were <1 mg/L, far lower than low-mineral water indicating mineralization of groundwater is effectively isolated from human impacts in surface environment (Fig. 1Sc (Supporting Material)). Low-mineral water and high-altitude springs displayed a decreasing trend of P_{CO2} with TDS, which is typical for a closed system with respect to soil CO_2 (Drever, 1997). The lower P_{CO2} in high-altitude springs could be attributed to the much weaker biological processes in the soil zone under colder climate. In contrast, CO_2-rich water and some mineral water had an elevated P_{CO2} of up to 1.1 MPa, even in conditions near equilibrium with respect to calcite, indicating the presence of additional CO_2 sources other than the soil zone, which were probably magmatic (Fig. 2). CO_2-rich water and some Na-type mineral water were saturated or slightly oversaturated with respect to calcite. The oversaturation is likely to be resulted from mixing of groundwater from different aquifer zones in the well bore which is near equilibrium at in situ conditions (Koh et al., 2009).

The sources of Cl and B in groundwater are atmospheric deposition and water–rock interactions when anthropogenic activities are negligible (Arnorsson and Andresdottir, 1995). It is known that B can be sorbed by Al and Fe oxides (Goldberg and Glaubig, 1985) and clay minerals (Goldberg and Glaubig, 1986). However, atmospherically derived B seems to be barely removed by the poorly developed soils of Jeju Island (Koh et al., 2005a). In this regard, B was evaluated as a possible indicator to degree of water–rock interactions. In the study area, Cl and B in recharge water were assumed to be derived mainly from marine aerosols with Cl/B mass ratio of 1330 (average seawater). For high-altitude recharge (RH), Cl concentration was assigned as 3.7 mg/L considering two high-altitude springs (>1000 m asl.). Cl concentration in mid-altitude recharge (RM) was determined as 6.2 mg/L considering low-
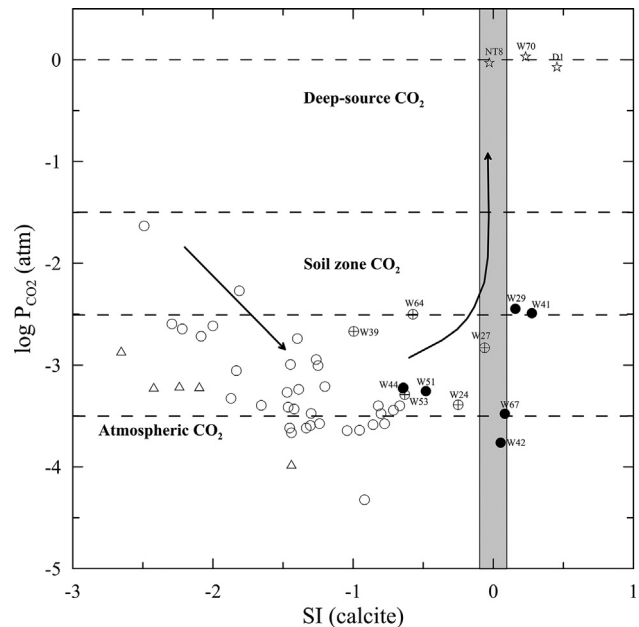

Fig. 2. P_{CO2} and saturation indices (SI) of calcite. Possible pathways of evolution in groundwater chemistry are shown as arrows.

mineral water with NO_3 <2.5 mg/L to minimize possible effect of anthropogenic sources (Koh et al., 2009).

Cl/B ratios showed a sharp decrease with increase of Cl concentration within the evolution envelope constructed considering ranges of concentrations of Cl and B in recharge waters and local basaltic rocks for most of samples while D1, the deepest well closely matched upper boundary of the evolution envelope (Fig. 3b). This indicates groundwater acquires B from interactions with basaltic rocks as mineralization progresses (Stefansson and Gislason, 2001). Two CO_2-rich waters (NT8 and W70) and some mineral waters had higher Cl/B ratios compared to the evolution zone assuming water–rock interactions which suggests these waters have additional Cl sources such as relic seawater as well as recharge water. Higher Cl concentration in some low-mineral water may be attributed to anthropogenic sources because they had slightly higher NO_3 concentration. The separation of low-mineral water and mineral water can be made at Cl/B ratios of 500–600, which provides another criterion for the extent of mineralization, as well as using the water type based on major ions and mineral content (Fig. 3b).

For identification of sources of salinity in groundwater, Br can be a useful indicator as ratios of Cl/Br (Vengosh and Pankratov, 1998; Alcala and Custodio, 2008). Though dissolved mineral content in groundwater are largely governed by bicarbonate concentration in this study, sources of Cl may provide useful information on hydrogeochemical processes. Cl/Br ratios of mineralized water are near that of seawater indicating sources of Cl are marine origin of either relict seawater during volcanic activity or sea-salt aerosols. Meanwhile, most of groundwater with NO_3 >about 3 mg/L showed Cl/Br ratios lower than that of seawater. Koh et al. (2009) suggested NO_3 > 2.5 mg/L may indicate anthropogenic effects in the study area and Koh et al. (2010) identified groundwater with lower Cl/Br ratios which is affected by agricultural activities in Korea. In this regard, groundwater with higher nitrate level is likely to have Cl sources other than marine sources.
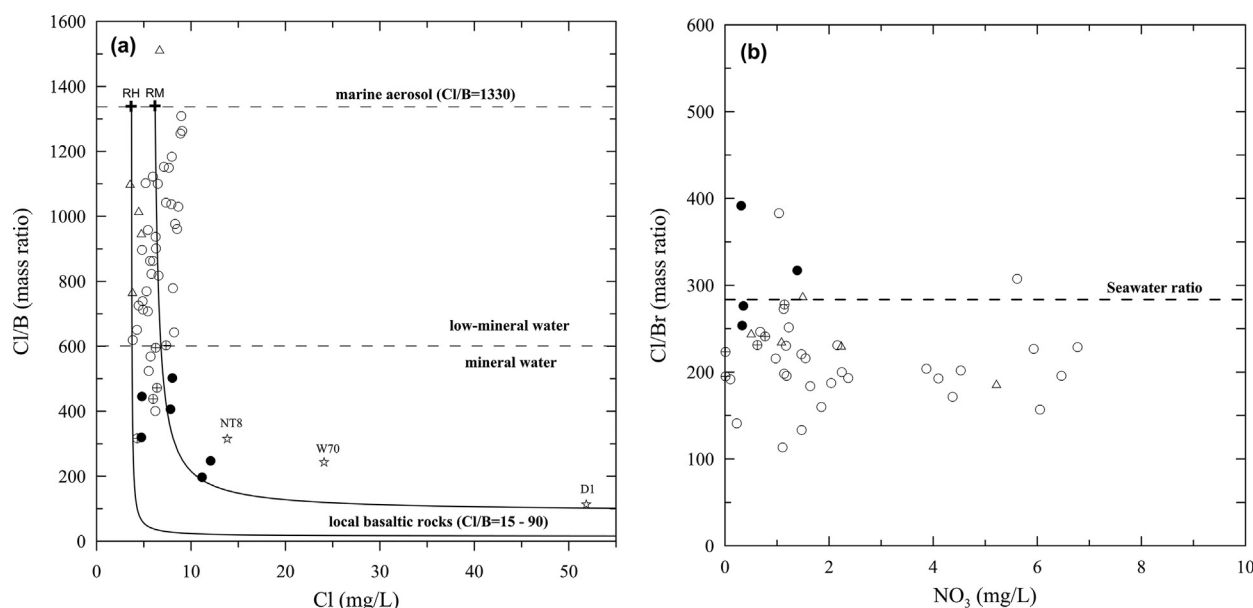
Fig. 3. Cl/B and Cl/Br ratios. (a) Cl/B mass ratios versus Cl concentration. An evolution envelope represents changes in Cl/B ratios and Cl concentrations in groundwater as recharge water dissolves Cl and B from the rock considering concentration ranges of Cl and B in recharge waters and local basaltic rocks. (b) Cl/Br mass ratios versus NO_3 concentration.

4.2. Silicate mineral-water equilibria

The saturation states of primary silicate minerals were evaluated to assess the potential reactivity of basaltic rocks with groundwater because the dissolution rates of minerals are dependent on the saturation states (Gislason and Arnorsson, 1993; Arnorsson et al., 2002). The solid solution compositions of silicate minerals in the basaltic rocks were presented for olivine, clinopyroxene, and plagioclase in phenocrysts and the groundmass by Koh et al. (2005b). The saturation index (SI) values of solid solutions were calculated by the approach of Aiuppa et al. (2000a, b) using the thermodynamic database, slop98. dat (http://geopig.asu.edu/supcrt92_data/slop98.dat) to calculate the free energies of dissolution reactions, and PHREEQC (Parkhurst and Appelo, 1999) to determine the ion activity products. The dissolution reactions used in the calculations are shown in Table 2. The Fe^{2+} concentration in water was assumed to be controlled by the solubility of amorphous $Fe(OH)_3$ under measured Eh conditions, because dissolved Fe was not detected or was present near the detection limit in most groundwater samples.

Groundwater was highly undersaturated with respect to the primary silicate minerals that comprise basaltic rocks (Fig. 4a). The SI values of olivine in phenocrysts and the groundmass were much lower than those of clinopyroxene and plagioclase. The saturation states increased as the water–rock interactions progressed. However, the undersaturation states were maintained even at the highest extent of mineralization. The decreased saturation states of

CO_2-rich water were due to the lower pH. The maintenance of undersaturation states with respect to primary silicate minerals indicates that the dissolution of basaltic rocks continued throughout the mineralization processes. The CO_2-rich water had a higher proportion of divalent cations than mineral waters, i.e., Mg for W70 and Ca for D1 (Fig. 1Sa (Supporting Material)). The highly undersaturated states of mafic primary minerals enabled the dominance of Ca and Mg over Na despite the near-saturation conditions with respect to calcite in CO_2-rich water (Fig. 4a).

To assess effects on concentration of dissolved silica, saturation states of groundwater with respect to silica minerals was compared. Groundwater is slightly oversaturated with chalcedony and slightly undersaturated with amorphous silica. However, concentration of dissolved silica in groundwater can be controlled by dissolution of glass or microcrystalline glassy materials in volcanic aquifers (Gislason and Eugster, 1987). In this regard, dissolved silica could be controlled by basaltic glass, not by chalcedony. Due to lack of data on chemical composition of basaltic glass in the island, evaluation of solubility equilibria with glass was not considered in this study.

Al concentration in groundwater seems to be controlled by gibbsite solubility because most of groundwater is near equilibrium with gibbsite though saturation states were scattered. However, mineral water was systematically undersaturated with gibbsite implying solubility control of Al by other solid phases such as kaolinite, halloysite and other clay minerals. Actually, all groundwater is highly oversaturated with kaolinite and smectites

Table 2
Dissolution reactions of primary silicate minerals in basaltic rocks.[a]

Olivine phenocrysts ($Fo_{0.74}$; $Fa_{0.27}$)
$(Mg_{0.74}Fe_{0.27})_2SiO_4 + 4H^+ \leftrightarrow 1.47Mg^{2+} + 0.53Fe^{2+} + SiO_2(aq) + 2H_2O$
Olivine in groundmass ($Fo_{0.66}$; $Fa_{0.34}$)
$(Mg_{0.66}Fe_{0.34})_2SiO_4 + 4H^+ \leftrightarrow 1.32Mg^{2+} + 0.68Fe^{2+} + SiO_2(aq) + 2H_2O$
Plagioclase ($An_{0.59}$; $Ab_{0.41}$)
$(Ca,Al)_{0.59}(Na,Si)_{0.41}AlSi_2O_8 + 6.36H^+ \leftrightarrow 0.59Ca^{2+} + 1.59Al^{3+} + 0.41Na^+ + 2.41SiO_2(aq) + 3.18H_2O$
Clinopyroxene ($En_{0.45}$; $Fs_{0.15}$; $Wo_{0.40}$)
$(Ca_{0.40}Mg_{0.45}Fe_{0.15})SiO_3 + 2H^+ \leftrightarrow 0.40Ca^{2+} + 0.45Mg^{2+} + 0.15Fe^{2+} + SiO_2(aq) + H_2O$

[a] Solid solution compositions are from Koh et al. (2005b).
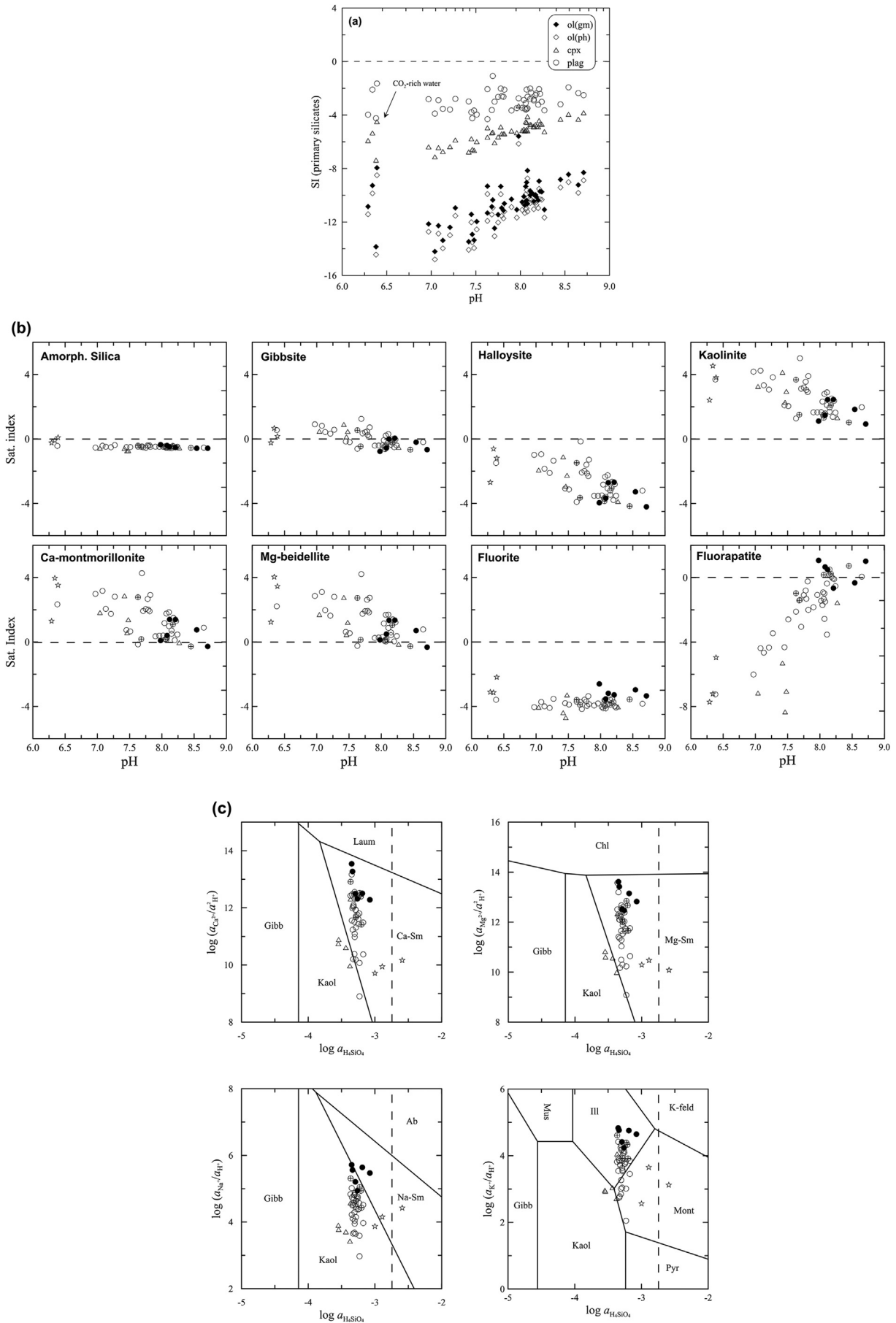
indicating these minerals could be formed during weathering of basaltic rocks (Gislason and Eugster, 1987). Meanwhile, groundwater is strongly undersaturated with respect to halloysite. This means kaolinite can be formed by transformation of halloysite precursors, which is suggested for a possible process of kaolinite formation (Fritz et al., 2009). However, slow kinetics of formation of these clay minerals could maintain higher oversaturation conditions in groundwater (Zhu, 2005; Maher et al., 2009). Therefore, dissolved Al concentration in considerable portion of the low-mineral water is unlikely to be controlled by precipitation of the clay minerals because low-mineral water has shorter residence time of 10–25 years (Koh et al., 2006). In contrast, mineral water has longer residence time (>50 years) than low-mineral water (Koh et al., 2009), which could explain undersaturation and much lower oversaturation states of mineral water with respect to gibbsite and kaolinite, respectively.

Smectites could regulate the concentrations of Al, Si, Ca, and Mg because most of the groundwater was in the stability field of Ca- and Mg-smectites, with smaller portion of samples on the boundaries of kaolinite and smectites (Fig. 4c), which was identified in previous works in the island (Koh et al., 2006) and Hawaiian islands (Nesbitt and Wilson, 1992). For K and silica, groundwater evolves along the boundary between kaolinite and montmorillonite, and that between illite and montmorillonite, and mineral water and considerable portion of low-mineral water are in the field of illite. This suggests that K is likely to be incorporated in illite (Garrels, 1984). In contrast, Na is the element least affected by the formation of clay minerals, and have a higher mobility during basaltic weathering (Banfield et al., 1991; Jeong and Sohn, 2011).

With the advancement of water–rock interactions, the formation of secondary minerals could be favored. Increases in the bicarbonate concentration and pH drove up the saturation states of calcite to oversaturation in some of the mineral water samples, including W41, W29, W42, W67, and W27 and CO_2-rich water. The loss of Ca compared to the other major cations in mineral water was attributed to the higher saturation with respect to carbonates (Koh et al., 2009; see also Fig. 2) which explains that Ca concentration increased at a lower rate in mineral water than in low-mineral water. Groundwater is also highly oversaturated with respect to smectite minerals (Fig. 4c). The formation of secondary silicate and carbonate minerals may also affect the behavior of trace elements by incorporating them in the exchange sites or by co-precipitation, which is discussed later.

Fluoride concentration is less than 0.4 mg/L in this study which is much lower compared to groundwater directly affected by active volcanoes (Aiuppa et al., 2000b; Stefansson et al., 2001). For example, F concentration in springs reached 5.1 mg/L near the active trachytic volcanoes in the volcanic island of São Miguel (Azores, Portugal) (Cordeiro et al., 2012). This is not surprising considering there is no active volcanic activity at present in the island. Compared to low-mineral water, Na-rich mineral water had higher F concentrations while Mg-rich mineral water had similar levels. This suggests F is likely to be supplied from dissolution of basaltic glass rather than mafic phenocrysts (Fig. 1Sb (Supporting Material)). Saturation states of F-bearing minerals indicate fluorite is unlikely to control F concentration (Fig. 4b). However, mineral water and some portion of low-mineral water are oversaturated with apatite indicating this mineral may control F concentrations if residence time of groundwater is sufficient to reach solubility equilibrium due to slow precipitation kinetics of apatite (Van Cappellen and Berner, 1991).

4.3. Trace elements in groundwater

Among the measured trace elements, Co, Ga, Ge, Se, Ag, Cd, Sn, Sb, Cs, Th, Be, Te, Ta, and Bi were not detected or were present at levels below the detection limit. The occurrence of these elements (except for Co and Th) might be negligible in groundwater simply due to the lower concentrations in aquifer materials that mainly consist of basaltic rocks (Taylor, 1965; Wedepohl, 1969). In contrast, B, Sc, Ti, V, Cr, Cu, Zn, Rb, Sr, Ba, Mo, and U were detected in the majority of samples. The measured concentrations of potentially toxic trace elements were compared with standards of EU drinking water directive (EU Directive, 1998/83/EC) and EU mineral water directive (EU Directive, 2003/40/EC). Concentrations of Mo, U, and V were compared with a health-based value (WHO, 2011), U.S. primary drinking water standard (US EPA, 2009), and the Italian legislation (D.M., 29/12/2003), respectively. For most of trace elements shown in Fig. 5, the measured concentrations were far below the standard values with only one sample exceeding the Italian standard for V. This indicates that the baseline conditions of groundwater quality controlled by dissolution of basaltic rocks in the study area are unlikely to cause health concerns for the elements.

There was a strong linear relation between the B and TDS over the various water types. The concentrations of alkali and alkaline earth elements also increased linearly with the increase in TDS (Fig. 2S). This indicates that concentrations of these elements are mainly controlled by dissolution of primary silicates. However, the rate of increase in the concentration of these elements was significantly damped in mineral water and CO_2-rich water, particularly for Rb and Ba. The concentration of Ba is likely to be affected by sinks including incorporation into secondary minerals like calcite and clay minerals, and adsorption to Fe–Mn oxyhydroxides (Aiuppa et al., 2000a).

The behavior of transition elements is strongly affected by pH during their interactions with oxides/hydroxides and carbonates (Dzombak and Morel, 1990; Zachara et al., 1991). The formation of oxyhydroxides greatly limits the aqueous concentrations of cationic trace elements in neutral to slightly alkaline conditions (Stumm and Morgan, 1996; Aiuppa et al., 2000a). The dissolved concentrations and solubility of oxyhydroxides were compared for Zn (Fig. 6). The Zn concentration was much lower than expected from the solubility of $ZnO_2(c)$, and smithsonite ($ZnCO_3$), in particular, for samples with a pH above 8.3. Sorption to iron and manganese oxides can effectively remove trace elements under alkaline conditions because these solid phases can be readily formed in oxidizing conditions during the chemical weathering of basaltic rocks. The sorption of Zn to iron oxides is therefore likely to increase under alkaline conditions, considering that the point of zero charge (pzc) of hydrous ferric oxide is about 8 (Dzombak and Morel, 1990). In mineral water, Zn is likely to be incorporated into precipitating calcite (Crocket and Winchester, 1966) or sorbed to calcite surfaces (Zachara et al., 1988) at conditions near equilibrium with calcite (Fig. 2).

The P concentration was widely scattered over the measured pH range (Fig. 6). The mobility of phosphates is greatly constrained by sorption on iron oxides and hydroxides in sediments (Ku et al.,

Fig. 4. Silicate mineral-water equilibria. (a) saturation indices (SI) of primary silicates versus pH, (b) SI of secondary minerals versus pH, and (c) activity–activity diagrams at 25 °C with P = 1 bar. Thermodynamic data were taken from Helgeson (1969) and Helgeson et al. (1978) for CaO–, MgO–, and $Na_2O–H_2O–SiO_2–Al_2O_3$ systems. A diagram for $K_2O–H_2O–SiO_2–Al_2O_3$ was from Garrels (1984). Mineral names were abbreviated as Gibb = Gibbsite, Kaol = Kaolinite, Sm = Smectite, Laum = Laumontite, Chl = Chlorite, Ab = Albite, Mus = Muscovite, Ill = Illite, K-feld = K-feldspar, Mont = Montmorillonite, and Pyr = Pyrophyllite. Vertical dash-dot lines are solubility of amorphous silica at 25 °C.
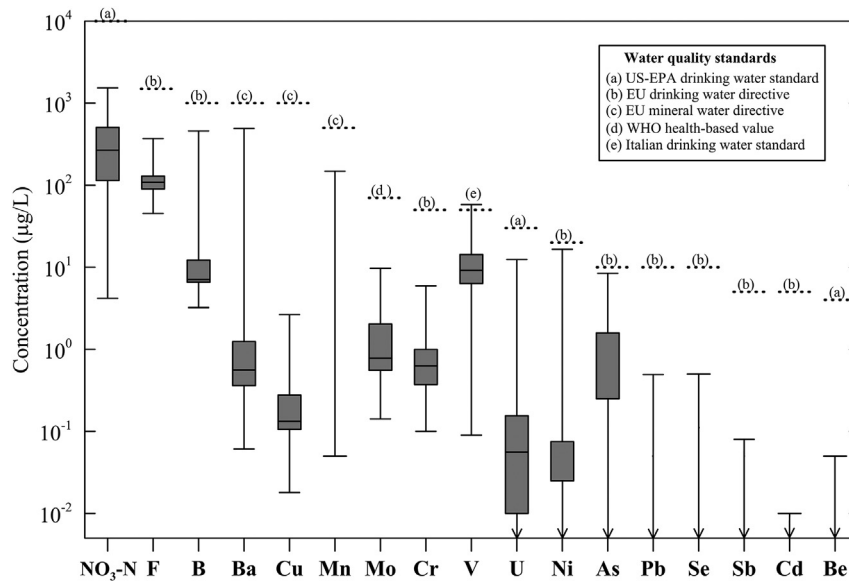
Fig. 5. Comparison of measured concentrations of potentially toxic elements in groundwater with various drinking water standards. Concentrations of Pb, Se, Sb, Cd, Ni, and As were below detection limits for most of samples. See text for the specific standard applied to each element.

1978; Spiteri et al., 2008). However, the lower level of P at higher pH, in particular for mineral water, could not be explained by adsorption to oxides, because the sorption of phosphates decreases at high pH (Stollenwerk, 1996). Instead, calcium-phosphate minerals can regulate P concentration in groundwater by solubility equilibrium with hydroxyapatite (Timperley, 1983) or fluorapatite (Vivona et al., 2007). Mineral water was oversaturated with respect to fluorapatite and near equilibrium with hydroxyapatite, as calculated using the average concentrations of Ca and F in mineral water (Fig. 2S). The Na-type mineral water had higher F concentration (maximum, 0.40 mg/L; median, 0.18 mg/L) compared to that of low-mineral water (median, 0.10 mg/L). The contrasting levels of P and F in Na-type mineral water suggest that dissolved P could be controlled by fluorapatite solubility, which was also identified in the saturation state of fluorapatite (Fig. 4b).

The sorption of oxyanions to oxides decreases with an increase of pH (Zachara et al., 1987; Dzombak and Morel, 1990), which may be applicable to V, excluding W29, which was anoxic (Fig. 6). Oxic-alkaline groundwater such as W42, W67, and W51 had higher concentrations of V, while more reduced and less alkaline groundwater, including W41, W29, and CO_2-rich water, had much lower concentrations, although the latter were more mineralized. This shows that a high pH also leads to higher V concentrations in groundwater, which may be due to the dominance of negatively charged vanadate above pH = 8 (Wright and Belitz, 2010). Compared to V, there were no clear trends in the Cr concentrations with an increase in the pH, and high concentrations were observed only at low pH.

4.4. Effect of redox conditions on trace elements

Redox conditions play a critical role in the occurrence and mobility of trace elements in groundwater (Frapporti et al., 1996; Smedley and Edmunds, 2002; Edmunds et al., 2003; Farnham et al., 2003). Groundwater in this study was mainly aerobic with a considerable DO content. The high DO could have resulted from the infiltration of rainfall through the highly permeable lava flows (Koh et al., 2006). The measured Eh levels also indicated oxygenated conditions, although they were slightly lower than expected

considering the high DO, which may be controlled by the redox of O_2/H_2O_2 due to the extremely slow kinetics of water oxidation (Langmuir, 1997). The negligible concentration of Fe and Mn in all samples was also indicative of the prevalence of aerobic conditions in the groundwater (Table 3S (Supporting Material)). The different behavior of some redox-sensitive elements was evaluated using Eh-pH diagrams.

The concentrations of V and Cr increased with the increase in TDS, although this trend was not clear in mineral water (Fig. 2S). Both V and Cr have the ability to form oxyanions in oxic conditions and their mobility is dramatically reduced in anoxic conditions due to the increased sorption and formation of insoluble solid phases (Aiuppa et al., 2000a; Wright et al., 2014). This is more pronounced for Cr, with very low concentration in most of the mineral water samples, while concentration of V was high in some mineral water, although the concentrations of both elements in basaltic rocks are positively correlated in Jeju Island (Park and Kwon, 1993b). This can be accounted for by the much larger stability fields of the insoluble Cr(III) oxides than V(IV) or V(III) oxides suggesting Cr-bearing solids are more favorably precipitated than V-bearing solids in reducing conditions. Measured Eh levels were near the boundary of Cr(VI)/Cr(III), while they were well above the boundary of V(V)/V(IV) or V(V)/V(III) (Fig. 7). This effect of high pH to suppress the increase of Cr but not V (Fig. 6) indicates the necessity to consider both redox and pH conditions.

The concentrations of Mo and U increased linearly with the increase in TDS for low-mineral water and some mineral water (Fig. 2S). The Eh conditions of most groundwater were well above the boundaries of the oxidized/reduced species, and highly mobile oxidized species of uranyl–carbonato complexes and molybdate were predominant (Fig. 7). In contrast, the concentrations of Mo and U decreased or increased at a much lower rate compared to the increase in TDS in anoxic groundwater and CO_2-rich water. The measured Eh values for these samples approached the stability fields of insoluble oxides and cationic species containing the elements, which provided favorable conditions for their removal from groundwater by sorption or precipitation of oxides.
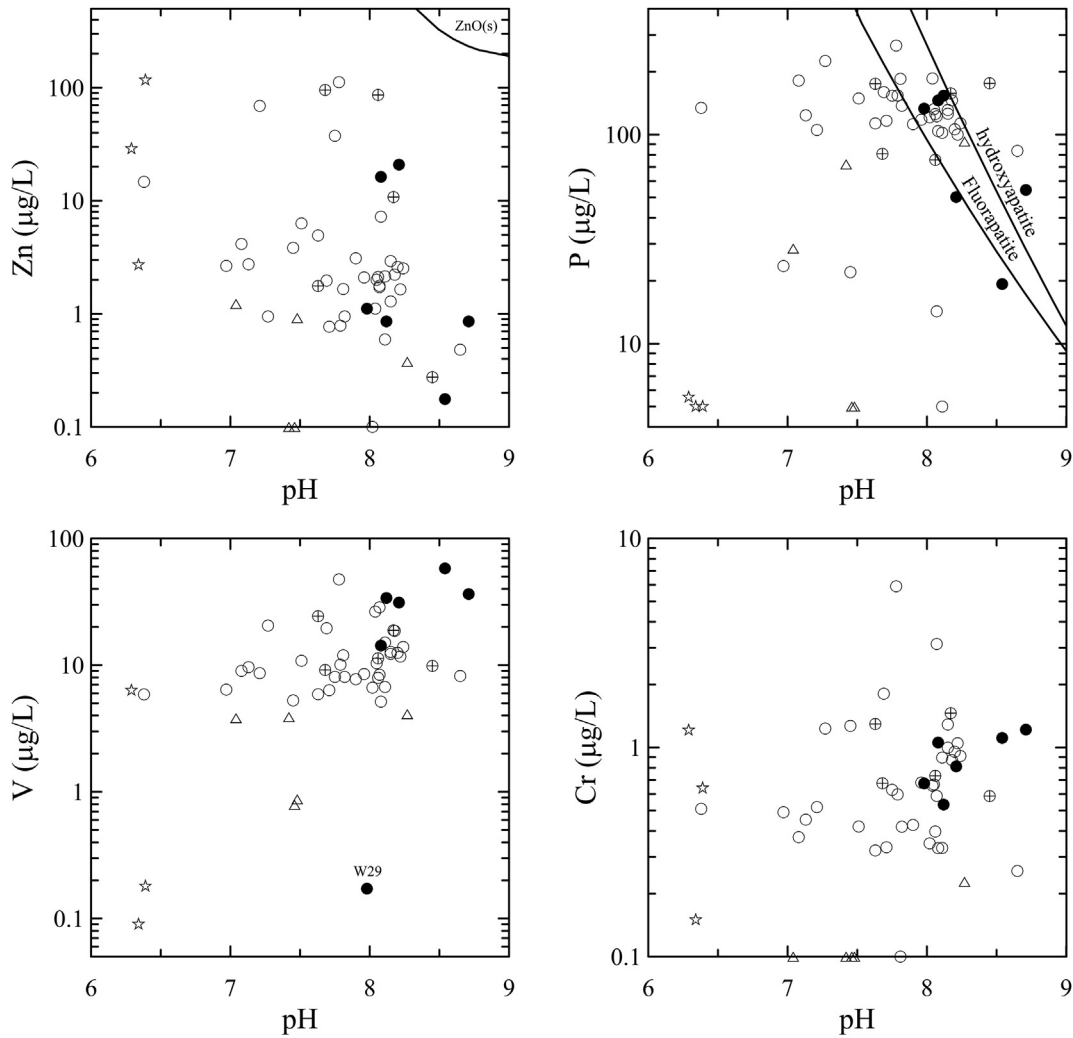
Fig. 6. Concentrations of Zn, P, V, and Cr versus pH. Thermodynamic data are from WATEQ4F database (Ball and Nordstrom, 1991).

4.5. Geochemical mobility of major and trace elements

The relative mobility (RM) of element X was calculated from their concentration ratios of water and fresh host rock, normalized to Na (Gislason et al., 1996; Aiuppa et al., 2000a):

$$RM = \frac{\left(\frac{X}{Na}\right)_{water}}{\left(\frac{X}{Na}\right)_{rock}} \tag{1}$$

To compare the mobility of each element in the aquifer conditions, the concentrations in groundwater were compared with those in the local basaltic rocks in Jeju Island (Table 1S (Supporting Material)), except for B and As whose contents in rocks were taken from average values in basalts (Taylor, 1965), because there is no data available for the local lithology. The median concentrations in low-mineral water and mineral water were regarded to be representative values for groundwater from the basaltic aquifers on the island. The effect of marine aerosols was corrected by assuming that the Cl concentration in recharge water was about 6 mg/L (Koh et al., 2009), which mostly affected Na and Mg. Among the trace elements, the concentrations of Li and As were highly variable, including considerable non-detections, and their mobility was very

uncertain. Both Th and Co were not detected in any samples, and were regarded as immobile (Fig. 8).

The oxyanion-forming elements (OXA); i.e., B and Mo, and alkali metals and alkaline earths (AAE) had a higher mobility, although the mobility of AAE varied widely with Na, K, and Rb being most mobile, Ca and Sr intermediate, and Ba being the least mobile. Compared to the other OXA, U had a relatively low mobility. The mobility of Si and P was similar to that of Sr. Among the first series transition metals (TRM), V, Sc, and Zn had relatively higher mobility, and Cr and Cu had lower mobility. In contrast, Co and Ni had much lower mobility compared to the other TRM. Al, Ti and Th were considered to be immobile, which is consistent with these elements being retained in refractory oxides. Using the RM, the elements could be grouped as: (1) mobile ($RM > 10^{-1}$) with B > Rb > Na > K > Mg > Ca > Mo > V > Si > Sr > Sc > P > U, (2) moderately mobile ($10^{-2} < RM < 10^{-1}$) with Zn > Pb > Cr > Cu, (3) slightly mobile ($10^{-3} < RM < 10^{-2}$) with Ba > Ni and, (4) immobile ($RM < 10^{-3}$) with Ti > Mn, Al, Fe, Th, and Co (Fig. 9).

4.6. Identification of geochemical processes using principal component analysis

From the principal component analysis of major and trace elements in groundwater, five principal components (PCs) were
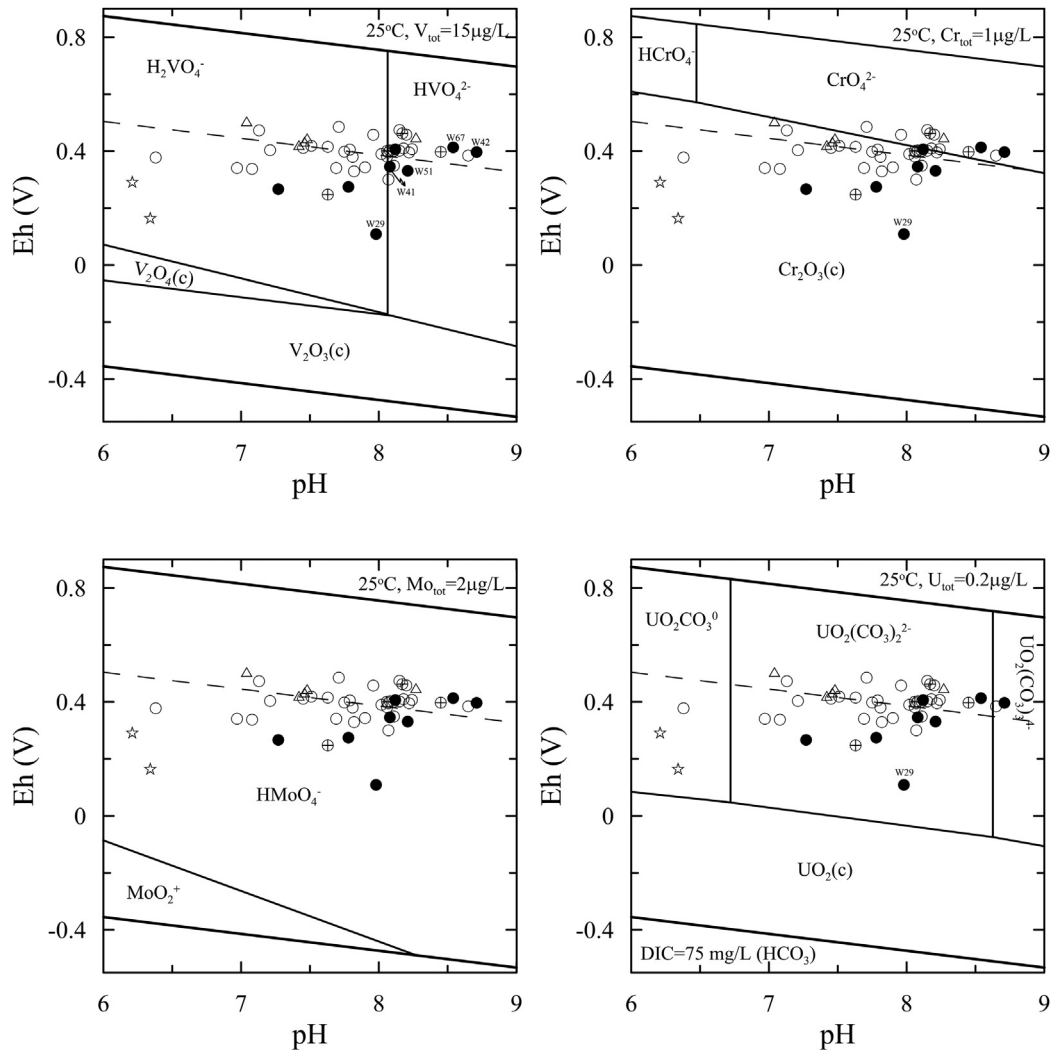
Fig. 7. Eh-pH diagrams of V, Cr, Mo, and U. Total concentrations are average values of low-mineral water and mineral waters. Thick solid lines are water stability limits and a dotted line is for the redox couple of O_2/H_2O_2 with $P_{O2}/a_{H2O2} = 10^6$ (Langmuir, 1997). Thermodynamic data for the trace elements are from Brookins (1988).

extracted using a Kaiser criterion and rotated by varimax method, which explained 82% of the total variance (Table 3). PC1 seems to mainly control occurrence of elements in groundwater because it explained nearly half of the total variance. It had higher positive loadings on TDS, HCO_3, and Cl and most of the remaining elements, and negative loadings on DO, NO_3, and P (Fig. 10a). B and Sr seem to behave similar to major cations because these elements were highly correlated in PC1 loadings. PC2 had higher positive loadings on V and Cr, and medium positive loadings on pH, DO, and Mo. V and Cr have similar geochemical characteristics in both rocks and groundwater (Aiuppa et al., 2000a, b) and Mo presents in groundwater as oxyanions like V and Cr in oxic conditions (Fig. 7). PC2 were typically represented by Na-type mineral water and the samples W36 and W66 among low-mineral water which have higher positive PC2 scores (Fig. 10b). In contrast, W29 and W70 have higher negative PC2 scores which are due to their anoxic conditions and lower V and Cr concentrations. PC3 had medium positive loadings on Cu, Zn, and Rb and medium negative loadings on Al, pH, and F. PC4 is correlated with Mo, Rb, and F while PC5 is linked positively with Ti and P and negatively with Eh.

In terms of spatial distribution, mineral water is concentrated in the southwestern areas, which was identified by Koh et al. (2009). CO_2-rich water is also found in that area indicating mineral water is

closely associated with CO_2-rich water (Fig. 3Sa (Supporting Material)). Spatial distribution of PC scores clearly showed major geochemical processes with distinct regional patterns integrating occurrence of major and trace elements in groundwater. Highest PC1 scores are concentrated in the southwestern area indicating higher degree of water–rock interactions supplying elements with higher mobility to groundwater (Fig. 3Sb (Supporting Material)). PC1 scores in the eastern and the western areas are also higher to a lesser extent, which is indicative of sizable effects of water–rock interactions. PC2 scores showed more scattered distribution compared to PC1 scores (Fig. 3Sc (Supporting Material)). Higher PC2 scores were observed in the western, northwestern, and eastern areas as well as the southwestern area, where alkaline conditions are prevalent due to higher degree of water–rock interactions still maintaining oxic conditions. Lower PC2 scores in the southwestern area are due to presence of anoxic groundwater in the area.

5. Discussion

5.1. Factors controlling the mobility of elements in groundwater

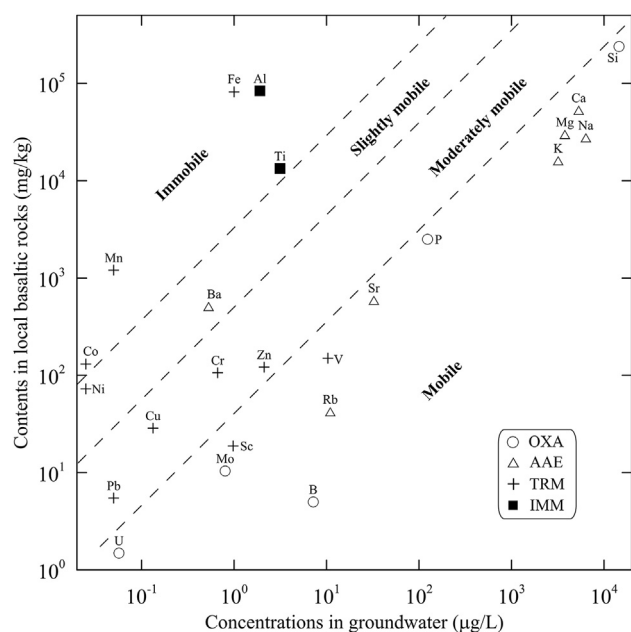The calculated mobility of elements varied widely, indicating

Fig. 8. Comparison of median concentrations of elements in groundwater (μg/L) and those in local basaltic rocks. Concentrations of elements in groundwater were corrected for the effect of marine aerosols. Elements are grouped as oxyanions (OXA), alkalis and alkaline earths (AAE), transition metals (TRM), and immobile elements (IMM).

that the interactions of water and volcanic rocks are not simple congruent reactions, but are affected by various processes that limit the elemental concentrations in groundwater (Aiuppa et al., 2000a; Parisi et al., 2011). With regard to the major elements, our results are in line with those of Stefansson and Gislason (2001), except for Ca, which had a mobility in the order of Na > Ca > Mg, K > Si >> Fe > Al in a study of a river and cold groundwater in Iceland. The reduced mobility of Ca in this study can be attributed to the large amount of plagioclase with labradorite composition in local basaltic rocks (Won, 1976; Koh et al., 2005b) because labradorite has a much lower dissolution rate than mafic minerals and volcanic glass (Drever, 1997; Wolff-Boenisch et al., 2004). It can be also attributed to the higher tendency for Ca to be retained in the solid phase during meteoric alteration of basaltic glass in the island compared to Na and Mg (Jeong and Sohn, 2011). These can be extended to explain the lower mobility of Sr than that of other alkalis and alkaline earths because Ca and Sr display similar behavior under many geochemical conditions. The mobility of P was high, similarly to Sr and V, and it is likely to exist mainly as HPO_4^{2-} at the measured pH conditions. The effect of P adsorption was weak in the basaltic aquifer due to the low surface area and alkaline conditions (pH = ~8) compared to sediments and soil zones.

For trace elements, the mobility calculated in this study was generally in line with the results of Aiuppa et al. (2000a, b) in an Etnean basaltic aquifer. However, some differences were also observed. The mobility of Fe and Mn in this study was lower than in the Etnean aquifer, which can be attributed to the formation of insoluble oxyhydroxides under oxic conditions, while Etnean groundwater had a considerable amount of anoxic water. The mobility of Ni, Co, and U was also lower compared to the Etnean aquifer. This may be explained by the higher pH conditions found in this study (average pH of 8.0) compared to those in Etnean groundwater (average pH of 6.8), which can significantly increase the sorption to oxides, such as hydrous ferric oxide. The much lower alkalinity also played a role in the lower mobility observed in

this study, because the predominant carbonato-complexes of the trace elements resulted in a higher mobility in Etnean groundwater. Compared to cold groundwater in a volcanic aquifer in Mount Vulture of the southern Italy (Parisi et al., 2011), mobility of V, Rb, and Sc in this study is higher and that of Fe and Mn is much lower. The differences in mobility of V, Fe, and Mn can be accounted for by more acidic (pH: 5.7 to 7.6) and more reducing (Eh: −41 to 298 mV) conditions of the Vulture aquifer than those in this study. Some specific samples were compared to the average mobility of elements in all groundwater samples. Anoxic groundwater (W29) had negative peaks of V and U and positive peaks of Fe and Mn compared to the average mobility, clearly indicating the effect of reducing conditions (Fig. 9a). Groundwater with pH > 8.5 (W67 and W42: high-pH water in Fig. 9a), had positive peaks of OXA, including V, U, and Mo, which indicates that the higher charged anions or more negatively charged surfaces increased the mobility of these elements. For V, Wright et al. (2014) also reported elevated concentration in oxic-alkaline groundwater controlled by adsorption/desorption reactions on mineral surfaces and much lower concentration in anoxic conditions resulted from precipitation of V-containing oxides in alluvial and volcaniclast deposits. Both anoxic and high-pH groundwaters had negative peaks of Zn, which indicates that Zn is selectively scavenged, possibly due to adsorption to secondary minerals such as iron oxides and calcite.

The CO_2-rich water had a highly fluctuating pattern of mobility compared to the average mobility of elements (Fig. 9b). Positive peaks were observed for Ba and Sr, which had comparatively lower mobility among the alkalis and alkaline earths in other samples. Carbonato-complexes of Ba and Sr are expected to be predominant based on much higher HCO_3 concentrations and lower pH decreases sorption, which increased the mobility of the elements. In contrast, mobility of P was lower, likely due to the increased sorption at a lower pH in CO_2-rich water (Stollenwerk, 1996). The strong negative peaks of V and U and positive peaks of Mn and Fe are likely to be the result of reducing conditions, which is similar to W29.

The results of PCA were useful to identify major geochemical processes controlling occurrence and mobility of major and trace elements in groundwater (Farnham et al., 2003). Jung et al. (2014) studied some trace elements including Fe, Mn, and V in groundwater from western coastal area of Jeju Island with intensive agricultural activities. They separated the effect of basalt weathering from agricultural contamination using PCA and identified that the weathering resulted in higher concentrations of Na, K, HCO_3, and V and higher pH in groundwater, which were refined into several specific processes in this study. The elements with higher mobility in the basaltic aquifers was highly correlated with PC1 which represents degree of mineralization, more specifically, dissolution of basaltic rocks by CO_2-charged water without significant attenuation of released solutes in the aquifers (Fig. 10a). PC2 accounted for the occurrence of redox sensitive oxyanions including V and Cr, and Mo and U to a lesser extent, which may indicate a process related to higher degree of water−rock interactions resulting in alkaline conditions with higher level of DO. This process is distinctively well represented by V which is close to pH and DO while other oxyanion-forming elements are closer to degree of mineralization in loading structures of PC1 and PC2 (Fig. 10a). These elements were also clearly distinguished from other trace elements in groundwater of alluvial aquifers with granite basement using PCA (Chen et al., 2007).

Other PCs are correlated with less number of parameters compared to PC1 and PC2. PC3 represents attenuation processes of Zn and Cu in higher pH which was clearly shown in Fig. 6. PC4 seems to be related to the dissolution of highly differentiated basaltic rocks because Rb is the most incompatible element in local
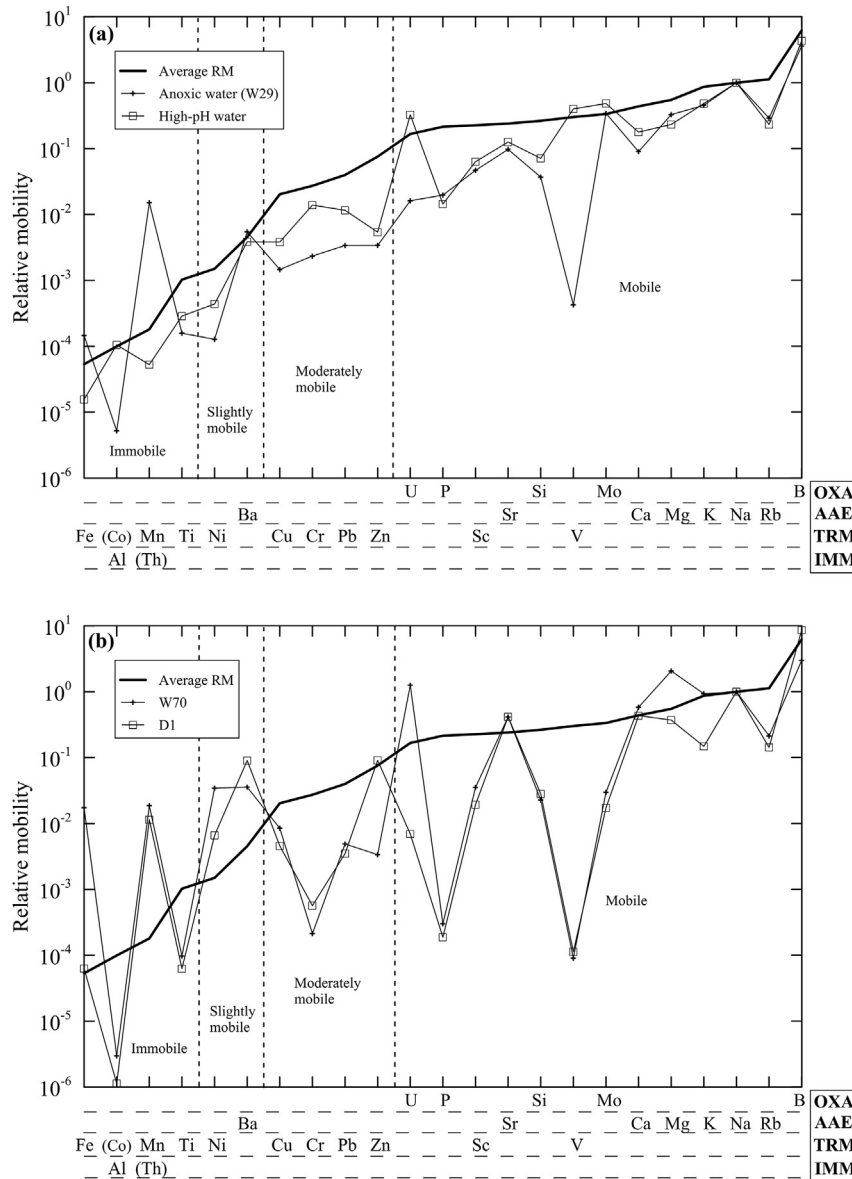
Fig. 9. Average relative mobility (RM) of elements normalized to Na in groundwater shown as a thick line. Element groups are arranged vertically by decreasing average mobility. Some specific samples are also shown as lines with symbols for comparison with the average RM. (a) anoxic and high-pH mineral water and (b) CO_2-rich water.

basaltic rocks (Park and Kwon, 1993b) and Mo and F are generally considered highly incompatible elements. PC5 could be attributed to release of Ti and P from Fe/Mn oxyhydroxides in anoxic conditions (Table 3).

5.2. Sources and sinks of TRM (V, Cr, Cu, and Zn) in groundwater

TRM with higher contents in the basaltic rocks had a very wide range of mobility, spanning those of alkaline earths and immobile elements, such as Al (Fig. 9). An evaluation of the sources and sinks in groundwater may provide insight into the mobility of these elements. Most trace elements in groundwater are acquired by the dissolution of minerals in the aquifers recharged by rainwater in the pristine area (Aiuppa et al., 2005). To determine the distribution of trace elements in groundwater, it is important to know which minerals in the rocks contain the elements, because dissolution rates are markedly different among minerals (Lasaga et al., 1994), and trace elements are selectively incorporated into specific

minerals (Soubrand-Colin et al., 2005). Because the trace element composition of minerals in the basaltic rocks in this study was not available, we used the partition coefficients between phenocrysts and the matrix determined for basaltic rocks in other areas to estimate the contents of trace elements in minerals. By considering the type of the basaltic rocks, the partition coefficients for alkali basalts were compiled for V, Cr, Cu, and Zn, with respect to olivine, clinopyroxene, plagioclase, and Fe−Ti oxides (Table 4).

Both V and Cr were estimated to be preferentially enriched in Fe−Ti oxides and clinopyroxenes, which are much more resistant to dissolution compared to glass and olivine. This indicates that the relatively higher mobility of V is due mainly to the higher mobility of oxyanions because the availability of the element from the rocks is low. The much lower mobility of Cr compared to V, may be attributed to sinks, such as the greater stability of Cr(III)-solids (Fig. 7), rather than sources in basaltic rocks because Cr and V have similar partitioning patterns between minerals and melts.

Copper in basaltic rocks has a higher affinity for glass with

Table 3
Principal component loadings rotated by varimax method.[a]

Variables	PC1	PC2	PC3	PC4	PC5	Communalities
Temp	0.69	*0.40*	−0.22	*0.14*	*0.11*	0.715
pH	*−0.30*	0.47	−0.45	*0.22*	*0.10*	0.574
EC	**0.97**	*0.04*	*0.14*	*0.18*	*−0.04*	0.988
DO	**−0.79**	0.40	*0.15*	*−0.20*	*−0.25*	0.906
Eh	−0.65	*0.22*	*0.25*	*−0.07*	−0.52	0.806
Ca	**0.93**	*−0.09*	*0.19*	*0.01*	*−0.19*	0.945
Mg	**0.92**	*−0.05*	*0.28*	*0.18*	*−0.06*	0.968
Na	**0.95**	*0.08*	*0.04*	*0.20*	*0.05*	0.956
K	**0.84**	*0.07*	*0.03*	*0.27*	*0.29*	0.864
HCO₃	**0.95**	*0.06*	*0.15*	*0.24*	*−0.04*	0.986
Cl	**0.85**	*−0.01*	*0.10*	*−0.38*	*0.06*	0.875
SO₄	**0.75**	*−0.08*	*0.03*	*−0.33*	*0.08*	0.683
NO₃	*−0.36*	*0.08*	*0.04*	**−0.84**	*−0.01*	0.841
F	*0.24*	*0.18*	−0.41	0.43	*0.39*	0.596
SiO₂	**0.77**	*0.05*	*0.30*	*0.12*	0.41	0.869
TDS	**0.96**	*−0.06*	*0.18*	*0.16*	*−0.01*	0.983
B	**0.93**	*0.12*	*0.00*	*0.22*	*0.15*	0.953
Al	*−0.02*	0.40	−0.66	*−0.12*	*0.24*	0.678
Ti	*0.07*	*0.06*	*−0.07*	*−0.03*	**0.84**	0.721
V	*−0.29*	**0.89**	*0.01*	*0.05*	*−0.02*	0.878
Cr	*0.29*	**0.84**	*−0.01*	*−0.04*	*0.16*	0.819
Cu	0.46	*0.01*	0.68	*−0.12*	*0.13*	0.700
Zn	*0.26*	*0.39*	0.62	*−0.08*	*0.07*	0.613
Rb	0.64	*−0.06*	0.42	0.43	*0.23*	0.830
Sr	**0.93**	*0.00*	*0.14*	*0.06*	*0.01*	0.894
Mo	0.55	0.40	*−0.21*	0.55	*0.32*	0.911
Ba	0.74	*−0.33*	*0.05*	*0.11*	*−0.02*	0.675
U	0.74	*0.22*	*0.25*	*0.36*	*−0.15*	0.819
Sc	**0.79**	*−0.05*	*0.33*	*0.18*	*0.16*	0.790
P	−0.41	*0.29*	*0.28*	*0.24*	0.67	0.848
Eigenvalue (λ)	14.55	2.91	2.57	2.33	2.31	–
% Variance explained	48.5	9.7	8.6	7.8	7.7	–
Cumulative % variance explained	48.5	58.2	66.8	74.6	82.3	–

[a] Loadings higher than 0.75 were shown as bold, those in range 0.40–0.75 in normal, and those lower than 0.40 are shown in italic fonts.
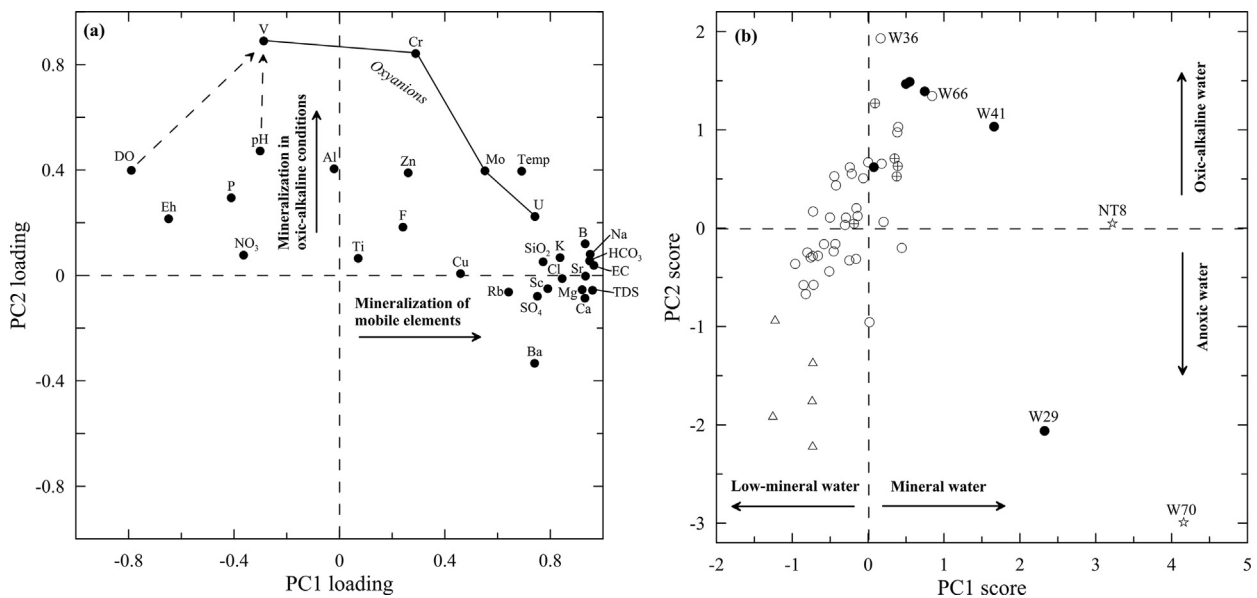

Fig. 10. Loadings and scores of principal components (PC). (a) PC1 loadings versus PC2 loadings and (b) PC1 scores versus PC2 scores.

respect to the major phenocrysts, which enables Cu to be effectively released to groundwater considering the higher proportion of glass in the basaltic rocks of the island (Park and Kwon, 1993b). This is contradicted by the relatively lower mobility of Cu in groundwater in this study, which may be accounted for by the higher sorption affinities of Cu for both hydrous iron oxides (Dzombak and Morel, 1990; Brown and Parks, 2002) and manganese oxides (Tonkin et al., 2004). This shows that both sources and sinks should be considered when determining the interactions of groundwater and aquifer materials for an element or species. The higher mobility of Zn compared to Cu can be also explained by this approach. Zinc has partitioning characteristics in rocks similar to Cu. However, Zn has

Table 4
Partition coefficients (K_d)[a] of transition metals between mineral-basaltic melts for alkali basalts.[b]

Element	Olivine		Clinopyroxene		Plagioclase		Fe–Ti oxides	
	K_d	Ref.	K_d	Ref.	K_d	Ref.	K_d	Ref.
V	0.06	5	2.2	4, 5	0.01	5	37	4
Cr	2.8	3	4.6	3, 5	0.08	3	4.2	3
Cu	0.07	1, 2	0.2	1, 2, 5	0.09	1, 2	0.9	1, 2
Zn	1.3	1, 2	0.5	1, 2	0.12	1, 2	1.5	1, 2

[a] If $K_d > 1$, the element is preferentially partitioned to the specified phenocryst mineral compared to basaltic melts and if $K_d < 1$, vice versa.
[b] References are 1. Bougault and Hekinian (1974), 2. Paster et al. (1974), 3. Villemant et al. (1981), 4. Chen et al. (1990), and 5. Hart and Dunn (1993). K_d values were averaged in case of multiple references.

lower sorption affinities for the hydrous oxides of Fe and Mn, which is likely to increase its mobility in groundwater.

5.3. Spatial correlation of water types and occurrence of elements in groundwater

Much higher P_{CO_2} levels of CO_2-rich water like W70 and NT8 could be evidence for existence of the deep CO_2 sources which were effectively isolated from nearby permeable aquifer zones (Fig. 3Sa (Supporting Material)). Also, occurrence of CO_2-rich water along with mineral water suggests that mineralization of groundwater is likely to be largely driven by supply of deep-seated CO_2 into the basaltic aquifer in the southwestern area. PC1 scores correlated with most of mobile elements showed linear alignment of higher scores along the NNE direction, which may indicate favorable conditions of water–rock interactions such as more mafic basaltic rocks encountered with CO_2-rich water (Fig. 3Sb (Supporting Material)). Meanwhile, distribution of PC2 scores is regionally corresponding to occurrence of oxic-alkaline groundwater, indicating spatial distributions of redox-sensitive elements are controlled by pH and redox conditions of groundwater as well as degree of mineralization (Fig. 3Sc (Supporting Material)). In particular, higher level of V and lower TDS in groundwater in the eastern area can be attributed to higher pH of that area (Wright and Belitz, 2010).

6. Conclusions

Groundwater from volcanic aquifers was largely of bicarbonate type and had a wide range of total dissolved solids (TDS) and P_{CO_2} from the weakly mineralized water with TDS of 50 mg/L to CO_2-rich water with TDS of 3400 mg/L in a predominantly natural area. Most of mineral water and CO_2-rich water was saturated with calcite and was located near the boundaries of kaolinite and smectites and within the illite field. In all samples, the groundwater was highly undersaturated with respect to olivine and clinopyroxenes, and plagioclase to a lesser extent, indicating that the dissolution of basaltic rocks could continue, with the precipitation of calcite and secondary silicates in highly mineralized water. The evolution envelope of B/Cl between marine aerosols and basaltic rocks fitted most of the groundwater well indicating that B could be a useful tracer of the interaction between water and basaltic rocks.

Among the measured trace elements, B, Al, P, Sc, Ti, V, Cr, Cu, Zn, Rb, Sr, Ba, Mo, and U were detected in the majority of groundwater samples. Redox-sensitive elements (V, Cr, Mo, and U) were affected by Eh-pH conditions to varying extents. The concentrations of V, Mo, and U linearly increased with the increase in mineralization and they only declined significantly in anoxic groundwater, likely due to the formation of insoluble solids for V and U, and the increased sorption of Mo under reducing conditions. Meanwhile, Cr concentration was lower in mineral water possibly due to the greater stability fields of the insoluble Cr solids compared to those of V although Cr behaved similarly to V in low-mineral water.

Relative mobility (RM) of elements revealed that oxyanion-forming elements and alkali metals had the highest mobility. Mobility of Ba was significantly lower while P and Si had intermediate mobility. Transition metals had a wide range of mobility with the mobility of V being at the higher end of the scale close to the alkaline earths, and Ni and Co being at the lower end of the scale corresponding to immobile elements. Zn had low mobility in groundwater saturated with calcite due to co-precipitation or sorption to carbonates. Compared to average RM, mobility of V and U was lower and that of Fe and Mn was higher in anoxic groundwater, and mobility of V was higher in oxic-alkaline water. In CO_2-rich water, Ba and Sr had relatively higher mobility and P had lower mobility due to the effect of elevated bicarbonate concentration and low pH, respectively.

Principal component analysis (PCA) showed that the elements with higher mobility were highly correlated with dissolution of basaltic rocks by CO_2-charged water without significant attenuation of released solutes in the aquifers and that V, Cr, and Mo were related to higher degree of water–rock interactions resulting in oxic-alkaline conditions. Attenuation of Zn and Cu in higher pH was also identified by PCA. V with higher mobility in groundwater was estimated to be enriched in Fe–Ti oxides and clinopyroxenes with lower dissolution rates. Zn and Cu had lower mobility in groundwater although both elements were estimated to be mostly present in basaltic glass with higher dissolution rates. This disparity between mobility and sources in rocks indicates that sinks are more important than sources in terms of controlling mobility of these elements in groundwater of basaltic aquifers. Elevated levels of most mobile elements like alkalis and alkaline earths in groundwater were concentrated in the southwestern area with a strong directional alignment while redox-sensitive elements like V had more complicated spatial distribution patterns, which is likely to be controlled by pH and redox conditions as well as degree of groundwater mineralization.

Appendix A. Supplementary data

Supplementary data related to this article can be found at http://dx.doi.org/10.1016/j.apgeochem.2015.11.004.

References

Aiuppa, A., Allard, P., D'Alessandro, W., Michel, A., Parello, F., Treuil, M., Valenza, M.,

2000a. Mobility and fluxes of major, minor and trace metals during basalt weathering and groundwater transport at Mt. Etna volcano (Sicily). Geochim. Cosmochim. Acta 64, 1827–1841.

Aiuppa, A., Dongarra', G., Capasso, G., Allard, P., 2000b. Trace metals in the thermal waters of Vulcano island. J. Volcanol. Geotherm. Res. 98, 189–207.

Aiuppa, A., Bellomo, S., Brusca, L., D'Alessandro, W., Federico, C., 2003. Natural and anthropogenic factors affecting groundwater quality of an active volcano (Mt. Etna, Italy). Appl. Geochem. 18, 863–882.

Aiuppa, A., Federico, C., Allard, P., Gurrieri, S., Valenza, M., 2005. Trace metal modeling of groundwater-gas-rock interactions in a volcanic aquifer: Mount Vesuvius, Southern Italy. Chem. Geol. 216, 289–311.

Alcalá, F.J., Custodio, E., 2008. Using Cl/Br ratio as a tracer to identify the origin of aquifers in Spain and Portugal. J. Hydrol. 359, 189–207.

Arnórsson, S., Andrésdóttir, A., 1995. Processes controlling the distribution of boron and chlorine in natural waters in Iceland. Geochim. Cosmochim. Acta 59, 4125–4146.

Arnorsson, S.N., Gunnarsson, I., Stefansson, A., Sveinbjornsdottir, A.E., 2002. Major element chemistry of surface and ground waters in basaltic terrain, N-Iceland. I. Primary mineral saturation. Geochim. Cosmochim. Acta 66, 4015–4046.

Ball, J., Nordstrom, D., 1991. User's manual for WATEQ4F with revised thermodynamic database and test cases for calculating speciation of major, trace and redox elements in natural waters. U.S. Geol. Surv. Water Resour. Investig. Rep. 91–183.

Banfield, J.F., Jones, B.F., Veblen, D.R., 1991. An AEM-TEM study of weathering and diagenesis, Abert Lake, Oregon: I. Weathering reactions in the volcanics. Geochim. Cosmochim. Acta 55, 2781–2793.

Bluth, G.J.S., Kump, L.R., 1994. Lithologic and climatic control of river chemistry. Geochim. Cosmochim. Acta 58, 2341–2359.

Bougault, H., Hekinian, R., 1974. Rift valley in the Atlantic Ocean near 36 degrees 50'N; petrology and geochemistry of basalt rocks. Earth Planet. Sci. Lett. 24, 249–261.

Brookins, D.G., 1988. Eh-pH Diagrams for Geochemistry. Springer, New York, p. 175.

Brown Jr., G.E., Parks, G.A., 2002. Sorption of trace elements on mineral surfaces: modern perspectives from spectroscopic studies, and comments on sorption in the marine environment. In: Ernst, W.G. (Ed.), Frontiers in Geochemistry: Organic, Solution, and Ore Deposit Geochemistry. Geological Society of America, Bellwether Publishing. Ltd.

Chen, C.-Y., Frey, F.A., Garcia, M.O., 1990. Evolution of alkalic lavas at Haleakala volcano, East Maui, Hawaii – major, trace element and isotopic constraints. Contrib. Mineral. Petrol. 105, 197–218.

Chen, K., Jiao, J.J., Huang, J., Huang, R., 2007. Multivariate statistical evaluation of trace elements in groundwater in a coastal area in Shenzhen, China. Environ. Pollut. 147, 771–780.

Cordeiro, S., Coutinho, R., Cruz, J.V., 2012. Fluoride content in drinking water supply in São Miguel volcanic island (Azores, Portugal). Sci. Total Environ. 432, 23–36.

Crocket, J.H., Winchester, J.W., 1966. Coprecipitation of zinc with calcium carbonate. Geochim. Cosmochim. Acta 30, 1093–1109.

Cruz, J.V., Amaral, C.S., 2004. Major ion chemistry of groundwater from perched-water bodies of the Azores (Portugal) volcanic archipelago. Appl. Geochem 19, 445–459.

EU Directive, 1998/83/EC. Council Directive of 3 November 1998 on the quality of water intended for human consumption 1998 Official Journal of the European Union L 330 32 5.12.1998.

EU Directive, 2003/40/EC. Council Directive of 16 May 2003 establishing the list, concentration limits and labeling requirements for the constituents of natural mineral waters and the conditions for using ozone-enriched air for the treatment of natural mineral waters and spring waters. Official Journal of the European Union L126/34 22/05/2003.

D.M, 29/12/2003. Decreto Ministero della Salute 29 dicembre 2003, attuazione della direttiva n. 2003/40/CE nella parte relativa ai criteri dei valutazione delle caratteristiche delle acque minerali naturali di cui al decreto ministeriale 12 .11.1992, n. 542, e successive modificazioni, nonché alle condizioni di utilizzazione dei trattamenti delle acque minerali naturali e delle acque di sorgente. Gazzetta Ufficiale n. 302 del 31-12-2003.

Drever, J.I., 1997. The Geochemistry of Natural Waters: Surface and Groundwater Environments, third ed. Prentice Hall, New Jersey, p. 436.

Dzombak, D.A., Morel, F.M.M., 1990. Surface Complexation Modeling: Hydrous Ferric Oxide. Wiley-Interscience, New York, p. 393.

Edmunds, W.M., Carrillo-Rivera, J.J., Cardona, A., 2002. Geochemical evolution of groundwater beneath Mexico City. J. Hydrol. 258, 1–24.

Edmunds, W.M., Guendouz, A.H., Mamou, A., Moulla, A.S., Shand, P., Zouari, K., 2003. Groundwater evolution in the continental intercalaire aquifer of Southern Algeria and Tunisia: trace element and isotopic indicators. Appl. Geochem 18, 805–822.

Farnham, I.M., Johannesson, K.H., Singh, A.K., Hodge, V.F., Stetzenbach, K.J., et al., 2003. Factor analytical approaches for evaluating groundwater trace element chemistry data. Anal. Chim. Acta 490, 123–138.

Fishman, M.J., Friedman, L.C., 1989. Methods for Determination of Inorganic Substances in Water and FLuvial Sediments (Book 5, Chapter A1). US Geological Survey Techniques of Water – Resources Investigations, p. 545.

Frapporti, G., Vriend, S.P., Gaans, P.F.M., 1996. Trace element in the shallow groundwater of the Netherlands. A geochemical and statistical interpretation for the nation monitoring network data. Aquat. Geochem 2, 51–80.

Fritz, B., Clement, A., Amal, Y., Noguera, C., 2009. Simulation of the nucleation and growth of simple clay minerals in weathering processes: the NANOKIN code.

Geochim. Cosmochim. Acta 73, 1340–1358.

Garrels, R.M., 1984. Montmorillonite/illite stability diagrams. Clay Clay Minerals 32, 161–166.

Giammanco, S., Ottaviani, M., Valenza, M., Veschetti, E., Principio, E., Giammanco, G., Pignato, S., 1998. Major and trace elements geochemistry in the ground waters of a volcanic area: Mount Etna (Sicily, Italy). Water Res. 32, 19–30.

Gislason, S.R., Arnorsson, S., 1993. Dissolution of primary basaltic minerals in natural waters: saturation state and kinetics. Chem. Geol. 105, 117–135.

Gislason, S.R., Eugster, H.P., 1987. Meteoric water-basalt interactions. II: a field study in N.E. Iceland. Geochim. Cosmochim. Acta 51, 2841–2855.

Gislason, S.R., Arnorsson, S., Armannsson, H., 1996. Chemical weathering of basalt in southwest Iceland: effects of runoff, age of rocks and vegetative/glacial cover. Am. J. Sci. 296, 837–907.

Goldberg, S., Glaubig, R.A., 1985. Boron adsorption on aluminum and iron oxide minerals. Soil Sci. Soc. Am. J. 49, 1374–1379.

Goldberg, S., Glaubig, R.A., 1986. Boron adsorption and silicon release by the clay minerals kaolinite, montmorillonite and illite. Soil Sci. Soc. Am. J. 50, 1442–1448.

Ha, K., Park, W.-B., Moon, D., 2009. Estimation of direct runoff variation according to land use changes in Jeju Island. Econ. Environ. Geol. 42 (4), 343–356.

Hart, S.R., Dunn, T., 1993. Experimental cpx/melt partitioning of 24 trace elements. Contrib. Mineral. Petrol. 113, 1–8.

Helena, B., Pardo, R., Vega, M., Barrado, E., Fernandez, J.M., Fernandez, L., 2000. Temporal evolution of ground water composition in an alluvial aquifer (Pisuerga River, Spain) by principal component analysis. Water Res. 34, 807–816.

Helgeson, H.C., 1969. Thermodynamics of hydrothermal systems at elevated temperatures and pressures. Am. J. Sci. 267, 729–804.

Helgeson, H.C., Delany, J.M., Nesbitt, H.W., Bird, D.K., 1978. Summary and critique of the thermodynamic properties of rock-forming minerals. Am. J. Sci. 278A, 1–229.

Jeong, G.Y., Sohn, Y.K., 2011. Microtextures, microchemistry, and mineralogy of basaltic glass alteration, Jeju Island, Korea, with implications for elemental behavior. Am. Miner. 96, 1129–1147.

Jeong, D., Yu, Y., Liu, Q., Jiang, Z., Koh, G.W., Koh, D.-C., 2014. Geomagnetic field intensity determination from pleistocene trachytic lava flows in Jeju Geopark. Geochem. Geophys. Geosyst. 15, 516–529.

Join, J.-L., Coudray, J., Longworth, K., 1997. Using principal components analysis and Na/Cl ratios to trace groundwater circulation in a volcanic island: the example of Reunion. J. Hydrol. 190, 1–18.

Jung, H.-W., Yun, S.-T., Kim, K.-H., Oh, S.-S., Kang, K.-G., 2014. Role of an impermeable layer in controlling groundwater chemistry in a basaltic aquifer beneath an agricultural field, Jeju Island, South Korea. Appl. Geochem 45, 82–93.

Kang, C.-H., Kim, W.-H., Hong, S.-B., Lee, K.-H., Hong, M.-S., Shim, S.-G., 1999. Analysis of rainwater in clean air area: characteristics of rainwater at 1100 site of Mt. Halla and Cheju City in 1997–1998 (in Korean). J. KOSAE 15, 555–566.

Kim, Y., Lee, K.-S., Koh, D.-C., Lee, D.-H., Lee, S.-G., Park, W.-B., Koh, G.-W., Woo, N.-C., 2003. Hydrogeochemical and isotopic evidence of groundwater salinization in a coastal aquifer: a case study in Jeju volcanic island, Korea. J. Hydrol. 270, 282–294.

Koh, D.-C., Chang, H.-W., Lee, K.-S., Ko, K.-S., Kim, Y., Park, W.-B., 2005a. Hydrogeochemistry and environmental isotopes of groundwater in Jeju volcanic island, Korea: implications for nitrate contamination. Hydrol. Process. 19, 2225–2245.

Koh, J.-S., Yun, S.-H., Hong, H.-C., 2005b. Morphology and petrology of Jisagae columnar joint on the Daepodong basalt in Jeju Island, Korea. J. Petrol. Soc. Korea 14, 212–225.

Koh, D.-C., Plummer, L.N., Solomon, D.K., Busenberg, E., Kim, Y., Chang, H.-W., 2006. Application of environmental tracers to mixing, evolution, and nitrate contamination of ground water in Jeju Island, Korea. J. Hydrol. 327, 258–275.

Koh, D.-C., Ko, K.-S., Kim, Y., Lee, S.-G., Chang, H.-W., 2007. Effect of agricultural land use on the chemistry of groundwater from basaltic aquifers, Jeju Island, South Korea. Hydrogeol. J. 15, 727–743.

Koh, D.-C., Chae, G.-T., Yoon, Y.-Y., Kang, B.-R., Koh, G.-W., Park, K.-H., 2009. Baseline geochemical characteristics of groundwater in the mountainous area of Jeju Island, South Korea: implications for degree of mineralization and nitrate contamination. J. Hydrol. 376, 81–93.

Koh, D.-C., Mayer, B., Lee, K.-S., Ko, K.-S., 2010. Land-use controls on sources and fate of nitrate in shallow groundwater of an agricultural area revealed by multiple environmental tracers. J. Contam. Hydrol. 118 (1–2), 62–78.

Ku, W.C., DiGiano, F.A., Feng, T.H., 1978. Factors affecting phosphate adsorption equilibria in lake sediments. Water Res. 12, 1069–1074.

Langmuir, D.A., 1997. Aqueous Environmental Geochemistry. Prentice-Hall, Upper Saddle River, NJ., p. 600

Lasaga, A.C., Soler, J.M., Ganor, J., Burch, T.E., Nagy, K.L., 1994. Chemical weathering rate laws and global geochemical cycles. Geochim. Cosmochim. Acta 58, 2361–2386.

Lee, M.-W., Won, C.-K., Lee, D.-Y., Park, G.-H., 1994. Stratigraphy and Petrology of volcanic rocks in Southern Cheju Island, Korea. J. Geol. Soc. Korea 30, 521–541.

Lee, K.-S., Wenner, D.B., Lee, I.-S., 1999. Using H- and O-isotopic data for estimating the relative contributions of rainy and dry season precipitation to groundwater: example from Cheju Island, Korea. J. Hydrol. 222, 65–74.

Louvat, P., Allegre, C.J., 1997. Present denudation rates on the island of Reunion determined by river geochemistry: basalt weathering and mass budget

between chemical and mechanical erosions. Geochim. Cosmochim. Acta 61, 3645—3669.

Maher, K., Steelel, C.I., White, A.F., Stonestrom, D.A., 2009. The role of reaction affinity and secondary minerals in regulating chemical weathering rates at the Santa Cruz soil Chronosequence, California. Geochim. Cosmochim. Acta 73 (10), 2804—2831.

Meybeck, M., 1987. Global chemical weathering of surficial rocks estimated from river dissolved loads. Am. J. Sci. 287, 401—428.

Moon, S.-H., Lee, J.-Y., Lee, B.-J., Park, K.-H., Jo, Y.-J., 2012. Quality of harvested rainwater in artificial recharge site on Jeju volcanic island, Korea. J. Hydrol. 414—415, 268—277.

Nesbitt, H.W., Wilson, R.E., 1992. Recent chemical weathering of basalts. Am. J. Sci. 292, 740—777.

Parisi, S., Paternoster, M., Perri, F., Mongelli, G., 2011. Source and mobility of minor and trace elements in a volcanic aquifer system: Mt. Vulture (southern Italy). J. Geochem. Explor. 110, 233—244.

Park, J.-B., Kwon, S.-T., 1993a. Geochemical evolution of the Cheju volcanic island: petrography and major element chemistry for stratigraphically-controlled lavas from the northern part of Cheju Island. J. Geol. Soc. Korea 29, 39—60.

Park, J.-B., Kwon, S.-T., 1993b. Geochemical evolution of the Cheju volcanic island (II): trace element chemistry of volcanic rocks from the northern part of Cheju Island. J. Geol. Soc. Korea 29, 477—492.

Park, J.-B., Park, K.-H., Cheong, C.-S., 1996. Sr-Nd-Pb isotopic compositions of lavas from Cheju Island, Korea. J. Petrol. Soc. Korea 5, 89—107.

Park, J.-B., Park, K.-H., Cho, D.-L., Koh, G.-W., 1999. Petrochemical classification of the quaternary volcanic rocks in Cheju Island, Korea. J. Geol. Soc. Korea 35, 253—264.

Park, C., Seo, J., Lee, J., Ha, K., Koo, M.-H., 2014. A distributed water balance approach to groundwater recharge estimation for Jeju volcanic island, Korea. Geosci. J. 18, 193—207.

Parkhurst, D.L., Appelo, C.A.J., 1999. User's Guide to PHREEQC (Version 2)-a Computer Program for Speciation, Batch-reaction, One-dimensional Transport, and Inverse Geochemical Calculations. WRI 99—4259. U.S. Geological Survey, Denver, p. 312.

Paster, T.P., Schauwecker, D.S., Haskin, L.A., 1974. The behavior of some trace elements during solidification of the skaergaard layered series. Geochim. Cosmochim. Acta 38, 1549—1577.

Pokrovsky, O.S., Schott, J., Kudryavtzev, D.I., Dupré, B., 2005. Basalt weathering in Central Siberia under permafrost conditions. Geochim. Cosmochim. Acta 69, 5659—5680.

Smedley, P.L., Edmunds, W.M., 2002. Redox patterns and trace element behaviour in the East Midlands triassic sandstone aquifer, UK. Ground Water 40, 44—58.

Sohn, Y.-K., Park, J.-B., Khim, B.-K., Park, K.-H., Koh, G.-W., 2002. Stratigraphy, petrochemistry and quaternary depositional record of the Songaksan tuff ring, Jeju Island, Korea. J. Volcanol. Geotherm. Res. 119, 1—20.

Soubrand-Colin, M., Bril, H., Néel, C., Courtin-Nomade, A., Martin, F., 2005. Weathering of basaltic rocks from the French Massif Central: origin and fate of Ni, Cr, Zn, and Cu. Can. Mineral 43, 1077—1091.

Spiteri, C., Cappellen, P.V., Regnier, P., 2008. Surface complexation effects on phosphate adsorption to ferric iron oxyhydroxides along pH and salinity gradients in estuaries and coastal aquifers. Geochim. Cosmochim. Acta 72, 3431—3445.

Stefánsson, A., Gíslason, S.R., 2001. Chemical weathering of basalts, southwest Iceland: effect of rock crystallinity and secondary minerals on chemical fluxes to the ocean. Am. J. Sci. 301, 513—556.

Stefánsson, A., Gíslason, S.R., Arnórsson, S., 2001. Dissolution of primary minerals in natural waters II. Mineral saturation state. Chem. Geol. 172, 251—276.

Stollenwerk, K.G., 1996. Simulation of phosphate transport in sewage-contaminated groundwater, Cape Cod, Massachusetts. Appl. Geochem. 11, 317—324.

Stumm, W., Morgan, J.J., 1996. Aquatic Chemistry, Chemical Equilibria and Rates in Natural Waters, third ed. John Wiley & Sons, Inc., New York, p. 1022.

Tatsumi, Y., Shukuno, H., Yoshikawa, M., Chang, Q., Sato, K., Lee, M.W., 2005. The petrology and geochemistry of volcanic rocks on Jeju Island: plume magmatism along the Asian continental margin. J. Petrol. 46, 523—553.

Taylor, S.R., 1965. The application of trace element data to problems in petrology. Phys. Chem. Earth 6 (C), 133—213.

Timperley, M.H., 1983. Phosphorus in spring waters of the Taupo volcanic zone, North Island, New Zealand. Chem. Geol. 38, 287—306.

Tonkin, J.W., Balistrieri, L.S., Murray, J.W., 2004. Modeling sorption of divalent metal cations on hydrous manganese oxide using the diffuse double layer model. Appl. Geochem. 19, 29—53.

US EPA, 2009. National Primary Drinking Water Regulations. EPA 816-F-09—0004. United States Environmental Protection Agency.

Van Cappellen, P., Berner, R.A., 1991. Fluorapatite crystal growth from modified seawater solutions. Geochim. Cosmochim. Acta 55, 1219—1234.

Van Der Weijden, C.H., Pacheco, F.A.L., 2003. Hydrochemistry, weathering and weathering rates on Madeira island. J. Hydrol. 283, 122—145.

Vengosh, A., Pankratov, I., 1998. Chloride/bromide and chloride/fluoride ratios of domestic sewage effluents and associated contaminated ground water. Ground Water 36 (5), 815—824.

Villemant, B., Jaffrezic, H., Joron, J.L., Treuil, M., 1981. Distribution coefficients of major and trace-elements - fractional crystallization in the Alkali Basalt Series of Chaine-Des-Puys (Massif Central, France). Geochim. Cosmochim. Acta 45, 1997—2016.

Vivona, R., Preziosi, E., Madé, B., Giuliano, G., 2007. Occurrence of minor toxic elements in volcanic-sedimentary aquifers: a case study in central Italy. Hydrogeol. J. 15, 1183—1196.

Wedepohl, K.H., 1969. Handbook of Geochemistry. Springer, Berlin, p. 442.

WHO, 2011. Guidelines for Drinking-water Quality, fourth ed. World Health Organization, Geneva.

Wolff-Boenisch, D., Gislason, S.R., Oelkers, E.H., Putnis, C.V., 2004. The dissolution rates of natural glasses as a function of their composition at pH 4 and 10.6, and temperatures from 25 to 74°C. Geochim. Cosmochim. Acta 68, 4843—4858.

Won, C.-K., 1976. Study of petro-chemistry of volcanic rocks in Jeju Island. J. Soc. Geol. Korea 12, 207—226.

Won, C.-K., Lee, M.-W., Yun, S.-H., Ko, B.-K., 1998. Geochemical characteristics of the volcanic rocks in Pyoseon area, southeast Cheju, Korea. J. Soc. Geol. Korea 34, 172—191.

Won, J.-H., Lee, J.-Y., Kim, J.-W., Koh, G.-W., 2006. Groundwater occurrence on Jeju Island, Korea. Hydrogeol. J. 14, 532—547.

Wright, M.T., Belitz, K., 2010. Factors controlling the regional distribution of vanadium in groundwater. Ground Water 48, 515—525.

Wright, M.T., Stollenwerk, K.G., Belitz, K., 2014. Assessing the solubility controls on vanadium in groundwater, northeastern San Joaquin Valley, CA. Appl. Geochem 48, 41—52.

Xie, Z.Q., Sun, L.G., Zhang, P.F., Zhao, S.P., Yin, X.B., Liu, X.D., Cheng, B.B., 2005. Preliminary geochemical evidence of groundwater contamination in coral islands of Xi-Sha, South China Sea. Appl. Geochem. 20, 1848—1856.

Zachara, J.M., Girvin, D.C., Schmidt, R.L., Thomas Resch, C., 1987. Chromate adsorption on amorphous iron oxyhydroxide in the presence of major groundwater ions. Environ. Sci. Technol. 21, 589—594.

Zachara, J.M., Kittrick, J.A., Harsh, J.B., 1988. The mechanism of Zn^{2+} adsorption on calcite. Geochim. Cosmochim. Acta 52, 2281—2291.

Zachara, J.M., Cowan, C.E., Resch, C.T., 1991. Sorption of divalent metals on calcite. Geochim. Cosmochim. Acta 55, 1549—1562.

Zhu, C., 2005. In situ feldspar dissolution rates in an aquifer. Geochim. Cosmochim. Acta 69, 1435—1453.